CrystEngComm

HIGHLIGHT

Cite this: *CrystEngComm*, 2016, **18**, 842

A brief review of the crucial progress on heterometallic polyoxotungstates in the past decade

Jiancai Liu, Qing Han, Lijuan Chen* and Junwei Zhao*

Received 4th December 2015,
Accepted 4th January 2016

DOI: 10.1039/c5ce02378e

www.rsc.org/crystengcomm

Heterometallic polyoxotungstates (HMPOTs) are still a challenging and attractive materials in polyoxometalate chemistry despite having generated remarkable interest in recent years not only on account of a variety of new structures and topologies but also because of their multiple potential applications in catalysis, magnetism, nanoscience, electrochemistry and photochemistry. This brief highlight article is principally focused on an overview of four types of HMPOTs: polyoxotungstate-based main-group (MG) and transition-metal (TM) heterometallic derivatives (PMGTMHDs), polyoxotungstate-based TM and TM heterometallic derivatives (PTMTMHDs), polyoxotungstate-based rare-earth (RE) and TM heterometallic derivatives (PRETMHDs) and polyoxotungstate-based RE and RE heterometallic derivatives (PREREHDs), and gives a summary of some representative examples involving their syntheses, structures and related properties. In addition, an outlook on these materials is also provided.

1 Introduction

Polyoxometalates (POMs) are a type of metal-oxo anionic clusters with a variety of structures and a wide range of important applications in catalysis, medicine, magnetism, optics, electrochemistry, and materials science.[1] Among POMs, lacunary Keggin- or Dawson-type polyoxotungstate (POT) clusters with higher negative charge and stronger coordination ability are usually utilized as excellent inorganic polydentate building units to link TM or RE cations to construct various TM-substituted POTs (TMSPs), RE-substituted POTs (RESPs) as well as PRETMHDs by exposing active coordination sites to their metal centers. These features affirmatively explain that POT chemistry is a continuously burgeoning research area and this fact is reflected in the number of published reports rapidly increasing in the past two decades, which almost covers every aspect of POT chemistry, from purely synthetic strategies primarily aiming at elucidating the mechanism of the assembly processes that governs POTs formation, to the applied research fields that attempt to expand the range of properties and applications of POTs. However, relevant reports on HMPOTs are very limited in contrast to a large number of already published monometallic POTs,

Henan Key Laboratory of Polyoxometalate Chemistry, Institute of Molecular and Crystal Engineering, College of Chemistry and Chemical Engineering, Henan University, Kaifeng, Henan 475004, PR China. E-mail: ljchen@henu.edu.cn, zhaojunwei@henu.edu.cn; Fax: (+86) 371 23881589

Jiancai Liu

Jiancai Liu was born in Henan Province, China and is studying for her MS degree in chemistry at Henan University in the group of Professor Junwei Zhao in Henan Key Laboratory of Polyoxometalate Chemistry. Her current research interest is concentrated on the preparation of novel organic–inorganic hybrid rare-earth-substituted polyoxometalate materials and their optical and electronic properties.

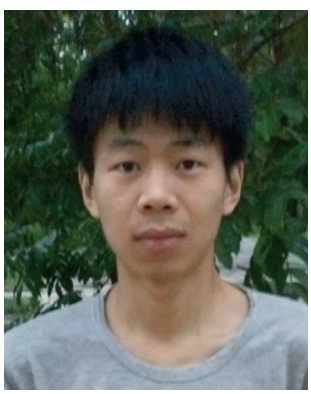

Qing Han

Qing Han was born in Henan Province, China. Currently, he is pursuing his MS degree at Henan University in Henan Key Laboratory of Polyoxometalate Chemistry under the supervision of Professor Junwei Zhao. His current research interest is focused on the designed synthesis and properties of polyoxometalates including transition metal and lanthanide clusters.

where it is comparatively difficult to precisely control the simultaneous aggregation of different metal cations in the POT system. To date, three typical synthetic methods have been used to obtain HMPOTs: (i) reaction of two types of metal cations with the simple tungstates;[2] (ii) introduction of two types of metal cations to the lacunary POT precursor system in the conventional aqueous solution or under hydrothermal conditions,[3] (iii) for lacunary POT precursors, first incorporate one type of metal cation giving rise to intermediates, and then the other type of metal cation is added to combine with intermediates.[4]

The first example of TMSP (an 11-tungstosilicate in which one tungsten atom of the Keggin structure is replaced by a Co^{2+} ion) was obtained by Simmons in 1962 and its structure was ultimately determined in 1966.[5,6] This discovery can be recognized as a great breakthrough in the realm of POT chemistry, which opens up an avenue to obtain attractive novel TMSP-based materials. Subsequently, this field underwent a rapid explosion as more and more researchers devoted great efforts to exploring this field. Hitherto, a large library of TMSPs have been reported.[7] Among the subfamily of POT, sandwich-type TMSPs constructed from two lacunary Keggin or Well–Dawson fragments anchoring a polynuclear metallic core have been extensively investigated and have been developed as the representative species since the first rhomb-like tetra-Co^{2+} sandwiched Keggin-type species $[Co_4(H_2O)_2(PW_9O_{34})_2]^{10-}$ was reported by Weakley *et al.* in 1973.[8] This series was further extended by replacing P^V with As^V, Si^{IV}, Ge^{IV}, As^{III}, Sb^{III}, Bi^{III}, Se^{IV} or Te^{IV} heteroatom followed by the formation of Well–Dawson sandwich-type TMSPs $[M_4(H_2O)_2(X_2W_{15}O_{56})_2]^{16-}$ (X = P^V and As^V; M = Co^{2+}, Cu^{2+}, and Zn^{2+}).[9] Because TM atoms in the belt can be replaced by one or two MG atoms, or by organometal (such as organotin) groups, a class of new derivatives was formed and named PMGTMHDs. The different approaches to obtain PMGTMHDs chiefly include: (i) incorporation of TM salts into lacunary Keggin or Well–Dawson precursors in the presence of high concentration of alkali metal salt in an aqueous solution, (ii) PMGTMHDs containing organometal groups are obtained by the reaction of lacunary POT precursors, TM ions and organometal groups, or alternatively, by the insertion of organometal groups to the prefabricated sandwiched TMSPs. It is worth noting that the first method is common to construct a sandwich-type PMGTMHDs with one or two exterior positions in the belt occupied by alkali metal ions. Sometimes these PMGTMHDs can be used as starting materials, in which alkali metal ions can be substituted by another TM ions to create PTMTMHDs. To the best of our knowledge, the first PTMTMHD $[Fe_4Cu_2W_{18}O_{70}H_6]^{10-}$ was discovered by Wasfi *et al.* in 1987.[10] From then on, the continuous interest in exploring PTMTMHDs has persisted and many reports have addressed their unique properties, which can be flexibly tuned *via* altering the type of the metal cluster in the sandwich belt (such as the number and the nature of metal atoms), as well as their potential applications in catalysis and electrocatalysis.[11]

The history of RESPs can be traced back to 1914 when Barbieri obtained the first RESP $(NH_4)_2[H_6CeMo_{12}O_{42}]\cdot nH_2O$.[12] However, the pioneer of RESPs should be ascribed to investigations on interactions of monovacant Keggin-type $[XW_{11}O_{39}]^{n-}$ (X = Si^{IV} and P^V) and Dawson-type $[P_2W_{17}O_{61}]^{10-}$ polyoxoanions with RE cations that were performed by Peacock and Weakley at the beginning of the 1970s.[13] In 2000, Pope *et al.* first reported two 1-D chain RESPs $\{Ln(\alpha\text{-}SiW_{11}O_{39})(H_2O)_3\}^{5-}$ (RE = La^{3+}, Ce^{3+}).[14] Subsequently, there was a significant increase in the number of reports on RESPs. In this research field, the self-assembly strategy of lacunary POT precursors and RE ions in the conventional aqueous

Lijuan Chen

Lijuan Chen was born in Henan, China. She gained her BS and MS degrees in chemistry from Henan University (2005) and obtained her PhD under the supervision of Professor Jianmin Chen at Lanzhou Institute of Chemical Physics, Chinese Academy of Sciences (2009). In 2009, she joined Henan University and was appointed as a lecturer. In 2013, she was promoted as an associate professor. Since April 2014, she has been working with Professor Jingyang Niu as a postdoctoral fellow in Henan University. Her research interest is focused on coordination chemistry and photophysical properties of polyoxometalate-based materials.

Junwei Zhao

Junwei Zhao obtained the BS degree in chemistry in 2002 and gained his MS degree under the supervision of Professor Jingyang Niu in 2005 from Henan University. In 2008, he received his PhD under the supervision of Professor Guo-Yu Yang at Fujian Institute of Research on the Structure of Matter, Chinese Academy of Sciences. After then, he became a faculty member of Henan University, was promoted to a full professor in chemistry in 2014 and was ranked as an academic leader of Department of Education of Henan Province and as a science & technology innovation talent in universities of Henan Province in 2015. He is mainly engaged in the synthesis and preparative chemistry of polyoxometalate-based functional materials and the relevant optical, electrical, magnetic and medical properties.

solution was developed as an effective and commonly used method.[15] Among the diverse POTs (Keggin, Dawson, Anderson, Weakley, and Lindqvist), lacunary Keggin- and Dawson-type POT precursors are conspicuously important partly because they are easily accessible and can be utilized as multidentate inorganic ligands to incorporate RE ions. Recently, based on the lone electron pair stereochemical effect of the heteroatoms, some heteroanion templates (SeO_3^{2-}, TeO_3^{2-}, and AsO_3^{3-}) were introduced to prepare high-nuclear RESPs.[16]

Although numerous TMSPs and RESPs have been extensively reported, the studies on PRETMHDs are relatively limited. The first examples of PRETMHDs go back to 2004 with the discovery of a series of $[RE(H_2O)_5\{Ni(H_2O)\}_2As_4W_{40}O_{140}]^{21-}$ (RE = Y^{3+}, Ce^{3+}, Pr^{3+}, Nd^{3+}, Sm^{3+}, Eu^{3+}, and Gd^{3+}) by Xue *et al.*[17] since then, intensive explorations have been continuously expanded, which were mainly focused on tungstophosphates,[18] tungstogermanates,[19] silicotungstates,[20] and tungstoarsenates.[21] Some representative results are illustrated in Scheme 1. It is well known that the unavoidable competitive reactions exist among highly negative POT precursors, strongly oxyphilic RE cations and less active TM cations in the same reaction system. Moreover, the combination of RE cations with POTs often easily results in precipitation rather than crystallization. Therefore, these facts make it difficult to obtain PRETMHD materials. Hence, seeking for the appropriate approaches to surmount the reaction drawbacks in the RE–TM–POT system is a great challenge. Hitherto, two main strategies were applied to prepare PRETMHDs, namely, the self-assembly reaction of simple starting materials or RE, TM ions and POT precursors with organic ligands and the stepwise assembly of pre-constructed precursors as building blocks and synthons. The stepwise assembly concretely includes three routes: the reaction of RE and TM heterometallic complexes as

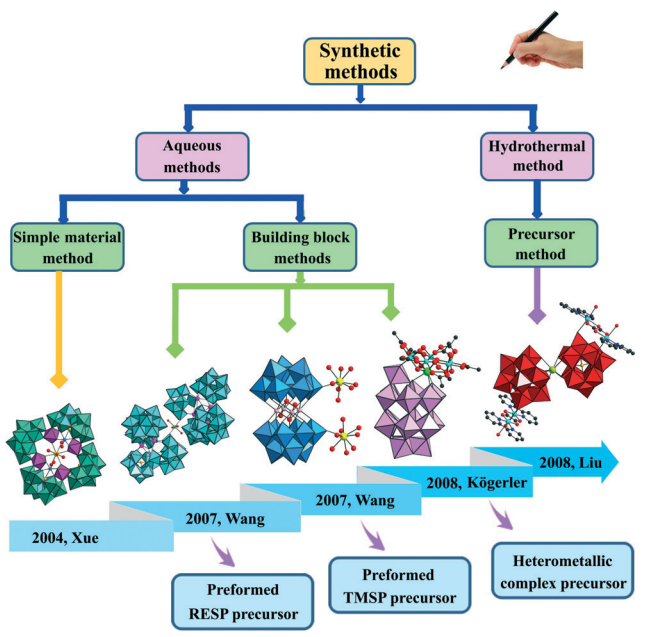

Scheme 1 Main synthetic methods to prepare PRETMHDs and the representative findings of each synthetic method.

precursors with POT precursors,[18a,b,20d] incorporation of TM ions to the preformed RESP precursors,[21a] and the incorporation of RE ions to the preformed TMSP precursors.[18i,19a,c,20f,g] These promising synthetic approaches have paved the way for synthesizing multifunctional PRETMHDs.

In the past decade, the POT chemistry has witnessed great progress on PRETMHDs with significant developments from purely inorganic aggregates to inorganic–organic hybrid extended architectures (*vide infra*). On the one hand, it is well known that the judicious choice of TM ions plays a vital role in the formation of predictable outcomes. Thus, in the RE–TM–POT system, researchers mainly concentrated their attention on Mn^{2+} and Cu^{2+} ions as well as slightly involved Fe^{3+} ions based on the following considerations: (i) Mn^{2+} ions can be easily oxidized to Mn^{3+} or Mn^{4+} by oxidants under alkaline conditions, and the incorporation of manganese ions in their intermediate oxidation states leads to interesting physicochemical properties that can be employed to synthesize a series of POT-containing catalysts due to their active redox catalytic activities; moreover, they have been extensively utilized to construct attractive magnetic aggregates, which is attributed to their relatively high spin values and negative single-axis magnetic anisotropy. (ii) In comparison with other TM ions, Cu^{2+} ions usually exhibit flexible coordination modes such as "square", "square-pyramidal", "trigonal bipyramidal" and "octahedral" geometries; besides, according to the crystal field theory, the d^9 electronic configuration of Cu^{2+} ions can be in the form of two electronic configurations: $(t_{2g})^6(d_{x2-y2})^2(d_{z2})^1$ or $(t_{2g})^6(d_{x2-y2})^1(d_{z2})^2$, leading to the flattened or elongated octahedral Cu^{2+} ion geometry of Cu^{2+} ions. The presence of the Jahn–Teller effect helps to overcome steric hindrance to form novel structures with high dimensionality and beautiful topologies. Therefore, they possess the prerequisite to be excellent synthons for constructing abundant coordination networks. On the other hand, the option of an organic ligands is also very important in creating PRETMHDs because elaborate organic ligands can combine with TM or RE ions forming metal–organic cations or directly function as connectors to enhance the stability of desired products. Therefore, N/O-including organic ligands such as aliphatic diamine ligands (en = ethylenediamine, dap = 1,2-diaminopropane) and aromatic ligands (2,2′-bpy = 2,2′-bipyridine, pzda = pyrazine-2,3-dicarboxylate), aminoacid ligand (thr = threonine), even to mixed ligands [2,2′-bpy and en, 2,2′-bpy and ox (oxalate)] are widely used. As for the synthetic methodology, apart from the traditional aqueous method, the hydrothermal synthetic technique was introduced to make inorganic–organic hybrid PRETMHDs. This technique has been deeply explored as an effective approach to make inorganic–organic hybrid TMSPs by Yang *et al.*,[22] where the high pressure and temperature of the hydrothermal conditions can efficiently increase the solubility of materials (insoluble organic ligands or precursors in an aqueous solution) and reduce the viscosity of solvents to improve the probabilities of various reaction components to obtain good-quality crystals.[23] With these two methods, a

variety of unprecedented PRETMHDs from isolated to polymers, from low-dimension to high-dimension, have already been obtained. This highlight article will comprehensively describe the major progress on PMGTMHDs, PTMTMHDs, PRETMHDs and PREREHDs with particular focus on the syntheses, structures and related properties of some representative compounds. Moreover, a personal outlook on the future development of HMPOTs is presented at the end.

2 The progress in PMGTMHDs

Commonly, trivacant Keggin and Well–Dawson lacunary POTs are widely used to prepare sandwich-type POTs with replacement of one or more adjacent high-valence tungsten centers by low-valence metal ions that can alter the electronic properties, which renders them to have attractive catalytic and electrochemical applications. It is worth noting that a high concentration of alkali metal ions plays a key role in stabilizing lacunary sandwich-type species. Therefore, by introducing lacunary precursors and TM salts into such a system with excess alkali metal ions, the exterior positions in the central belt of the resulting TMSPs can be replaced by one or two alkali metal ions, leading to some interesting PMGTMHDs.[24a–l] Overall, the reported tetranuclear sandwiched PMGTMHDs prevailingly contain two types of $\{M_3M'(XW_9O_{34})_2\}/\{M'_3M(X_2W_{15}O_{56})_2\}$ (ref. 24*a–f*) and $\{M'_2M_2(XW_9O_{34})_2\}/\{M'_2M_2(X_2W_{15}O_{56})_2\}$ (ref. 24*g–l*) (M = Na^+ or Li^+, M′ = TM). For instance, by treating $[A\text{-}PW_9O_{34}]^{9-}$ anions with Ni^{2+} ions in aqueous sodium, Kortz and coworkers successfully isolated a dimeric PMGTMHD $[Ni_3Na(H_2O)_2(PW_9O_{34})_2]^{11-}$ (Fig. 1a), featuring two lacunary Keggin $[B\text{-}PW_9O_{34}]^{9-}$ moieties linked by a rhomb-like $\{Ni_3NaO_{16}\}$ group where two Ni^{2+} ions reside in the two inner positions, whereas the two outer positions are occupied by a Na^+ ion and a Ni^{2+} ion.[24a] Its electrochemical behaviors displayed a stable and reproducible voltammetric pattern with a first wave undergoing a chemically reversible four-electron process, exhibiting very promising catalytic activity. Hill *et al.* synthesized a Dawson-type PMGTMHD $[Fe^{III}_2(NaOH_2)_2(P_2W_{15}O_{56})_2]^{16-}$ (Fig. 1b) by sandwiching a central $\{Fe_2Na_2\}$ core, where two Na^+ ions were located in the external positions and two Fe^{3+} ions resided in the internal positions.[24g] This compound acts as a high-efficiency catalyst for a H_2O_2-based epoxidation reaction, which exhibits high selectivity toward the oxidation of alkenes. Besides the common tetra-nuclear dimeric PMGTMHDs, penta- and hexa-nuclear sandwich-type PMGTMHDs have also been reported.[24m–v] In 2013, Hill *et al.* synthesized a dicobalt-containing silicotungstate $[\{Na_3(\mu\text{-}OH_2)_2Co_2(\mu\text{-}OH)_4\}(Si_2W_{18}O_{66})]^{13-}$ (Fig. 1c) by the reaction of Co^{2+} cations with $[A\text{-}\alpha\text{-}SiW_9O_{34}]^{10-}$ anions in sodium acetate buffer of pH = 4.8 and showed that two Co^{2+} and three Na^+ ions were encapsulated in the central pocket of the $[Si_2W_{18}O_{66}]^{16-}$ anion.[24m] Similarly, another penta-nuclear $[K_2\{Co(H_2O)_2\}_3(SiW_9O_{34})_2]^{12-}$ (Fig. 1d) was obtained by Hervé *et al.*, which consisted of two $[A\text{-}\alpha\text{-}SiW_9O_{34}]^{10-}$ connected by three Co^{2+} and two K^+ cations.[24n] Zhao *et al.* and Kortz *et al.* isolated hexa-nuclear $[Cu(en)_2(H_2O)]_4[Cu(en)_2(H_2O)_2][Cu_2Na_4(\alpha\text{-}SbW_9O_{33})_2]\cdot 6H_2O$ (Fig. 1e)[24o] and $[(\alpha\text{-}SbW_9O_{33})_2Cu_3(H_2O)_3Na_3(H_2O)_6]^{9-}$ (Fig. 1f),[24p] respectively, in which two $[(\alpha\text{-}SbW_9O_{33})]^{9-}$ units were linked by a hexa-atomic ring defined by Cu^{2+} and Na^+ ions. The related hexa-nuclear $[Cs_2Na(H_2O)_{10}Pd_3(\alpha\text{-}SbW_9O_{33})_2]^{9-}$ (Fig. 1g) containing two types of MG atoms and one type of TM atom was also discovered by the Kortz group,[24t] which represented the first example of PMGTMHD containing a 2p–4d–5p elements. The cyclic voltammetry (CV) in the acetate buffer solution of pH = 5 results in the deposition of a Pd^0 film on the glassy carbon electrode surface from Pb^{2+} ions in $[Cs_2Na(H_2O)_{10}Pd_3(\alpha\text{-}SbW_9O_{33})_2]^{9-}$. An especially hydrogen sorption/desorption peak observed in CV curve indicates the good quality of the Pd^0 film.[24t] Some other examples of Pd-substituted PMGTMHDs are well described in $[Cs_2K(H_2O)_7Pd_2WO(H_2O)(A\text{-}\alpha\text{-}SiW_9O_{34})_2]^{9-}$ and $[Cs_2Na(H_2O)_8Pd_3(\alpha\text{-}AsW_9O_{33})_2]^{9-}$.[24u,v]

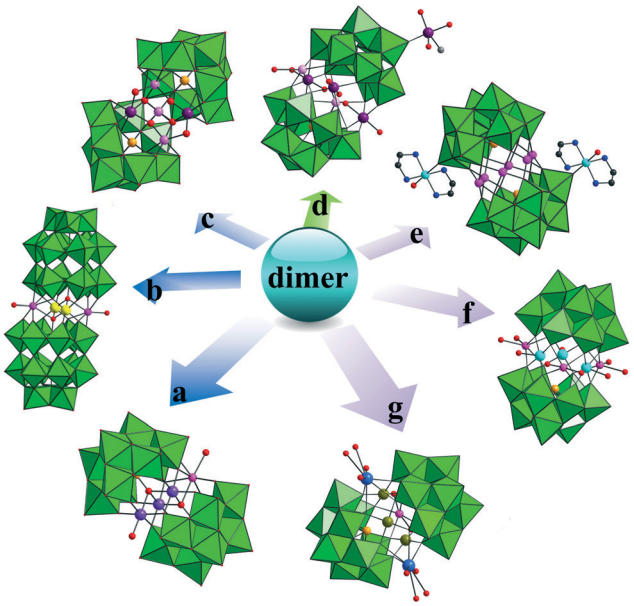

Fig. 1 Some typical dimeric sandwich-type PMGTMHDs. View of (a) $[Ni_3Na(H_2O)_2(PW_9O_{34})_2]^{11-}$ [Ni: purple], (b) $[Fe^{III}_2(NaOH_2)_2(P_2W_{15}O_{56})_2]^{16-}$ [Fe: yellow], (c) $[\{Na_3(\mu\text{-}OH_2)_2Co_2(\mu\text{-}OH)_4\}(Si_2W_{18}O_{66})]^{13-}$ [Co: violet], (d) $[K_2\{Co(H_2O)_2\}_3(SiW_9O_{34})_2]^{12-}$ [Co: violet, K: rose], (e) $[Cu(en)_2(H_2O)]_4[Cu(en)_2(H_2O)_2][Cu_2Na_4(\alpha\text{-}SbW_9O_{33})_2]\cdot 6H_2O$ [Cu: turquiose; CuNa: pink], (f) $[(\alpha\text{-}SbW_9O_{33})_2Cu_3(H_2O)_3Na_3(H_2O)_6]^{9-}$ [Cu: turquiose] and (g) $[Cs_2Na(H_2O)_{10}Pd_3(\alpha\text{-}SbW_9O_{33})_2]^{9-}$ [Pd: dark yellow; Cs: light blue].WO_6: bright green, Na: rose-bengal, O: red, C: gray, N: blue, X: light orange.

Though purely inorganic sandwich-type PMGTMHDs have been well documented and characterized, the inorganic–organic hybrid dimeric PMGTMHDs with organometal fragments remain limited.[25] In 2014, Wang's group obtained the first inorganic–organic hybrid PMGTMHD functionalized by open chain carboxyltin groups $[Mn_2\{Sn(CH_2)COOH\}_2(B\text{-}\alpha\text{-}GeW_9O_{34})_2]^{10-}$ (Fig. 2a) by reacting $Cl_3Sn(CH_2)_2COOCH_3$ with the Mn_4-sandwiched $Na_{12}[Mn_4(H_2O)_2(GeW_9O_{34})_2]\cdot 38H_2O$,[25a] which displayed the well-known sandwich-type structural

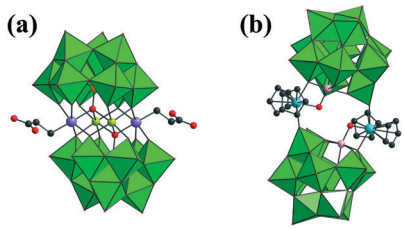

Fig. 2 (a) View of $[Mn_2\{Sn(CH_2)COOH\}_2(B\text{-}\alpha\text{-}GeW_9O_{34})_2]^{10-}$ [Mn: lime, Sn: purple], (b) view of $\{[\alpha\text{-}PW_{11}Al(OH)O_{39}ZrCp_2]_2\}^{6-}$ [Al: rose, Zr: aqua]. WO_6: bright green, O: red, C: gray-80%, N: blue, X: light orange.

feature with two Mn^{2+} cations and two $[Sn(CH_2)_2COOH]^{3+}$ segments encapsulated in the internal and external positions in the central belt. It is worth noting that the estertin precursor $[Sn(CH_2)_2COOCH_3]^{3+}$ as a starting material hydrolyzes into carboxyltin $[Sn(CH_2)_2COOH]^{3+}$ containing a newly exposed carboxyl group, which can combine with organic groups or metal cations during the reaction process; this not only allows further functionalization of carboxyltin decorated POTs, but also provides a guarantee for the loading of POTs onto the surface of TiO_2. Some analogical structures were also addressed by his group as well as Zhu's group.[25b–d] Moreover, Kato *et al.* obtained a mono-Al-substituted Keggin dimer with zirconocene linkers $\{[\alpha\text{-}PW_{11}Al(OH)O_{39}ZrCp_2]_2\}^{6-}$ (Fig. 2b) by the reaction of mono-Al-substituted phosphotungstate $[(n\text{-}C_4H_9)_4N]_4[\alpha\text{-}PW_{11}\{Al(OH_2)\}O_{39}]$ with $Cp_2Zr(OTf)_2{\cdot}THF$ (OTf = $O_3SCF_3^-$) in acetonitrile, which is made up of two $\{PW_{11}AlO_{40}\}$ units bridged by "bent sandwich" $\{ZrCp_2\}$ segments with C_2 symmetry.[25e] Furthermore, the Fourier transform infrared spectra and the solution nuclear magnetic resonance spectra indicated that this complex is highly stable in acetonitrile.

Besides these dimeric PMGTMHDs, in 2008, Wei *et al.* reported two 1-D organic–inorganic hybrids $[\{Cu(im)_4\}\{Na(H_2O)_2\}_3\{Cu_3(im)_2(H_2O)\}(XW_9O_{33})_2]_{2n}$ (X = Bi^{III} and Sb^{III}) (Fig. 3a),[26a] constructed from sandwich-type $[\{Na(H_2O)_2\}_3\{Cu_3(im)_2(H_2O)\}(XW_9O_{33})_2]^{9-}$ subunits and $[Cu(im)_4]^{2+}$ bridging cations. In the central belt of the sandwich-type anion, three hexa-coordinate Na^+ ions together with three penta-coordinate Cu^{2+} ions are located in an alternating mode, furnishing a six-member ring. Interestingly, adjoining sandwich-type polyoxoanions were connected together by $[Cu(im)_4]^{2+}$ ions into an 1-D line chain alignment running along the [1 0 −1] direction (Fig. 3b).[26a] In the same year, Niu's group obtained a series of sandwich-type complexes through the self-assembly of Sb_2O_3 and $Na_2WO_4{\cdot}2H_2O$ or $(NH_4)_{18}[NaSb_9W_{21}O_{86}]$ with TM ions (TM = Mn^{2+} and Cu^{2+}) in an aqueous solution.[26b] Among these, the structure of $[Na_3(H_2O)_6Mn_3(\mu\text{-}CH_3COO)_2(B\text{-}\alpha\text{-}SbW_9O_{33})_2]^{11-}$ (Fig. 3c) is extremely similar to that of the sandwich-type $[\{Na(H_2O)_2\}_3\{Cu_3(im)_2(H_2O)\}(SbW_9O_{33})_2]^{9-}$ subunit observed in $[\{Cu(im)_4\}\{Na(H_2O)_2\}_3\{Cu_3(im)_2(H_2O)\}(SbW_9O_{33})_2]_{2n}$,[26a] which comprises a hexa-atomic ring defined by three Na^+ ions and three Mn^{2+} ions alternately, giving rise to a sandwich-type structure.[26b] A striking difference between them is that the im ligands in $[\{Na(H_2O)_2\}_3\{Cu_3(im)_2(H_2O)\}(SbW_9O_{33})_2]^{9-}$ just partially substitute the water molecules and participate in the

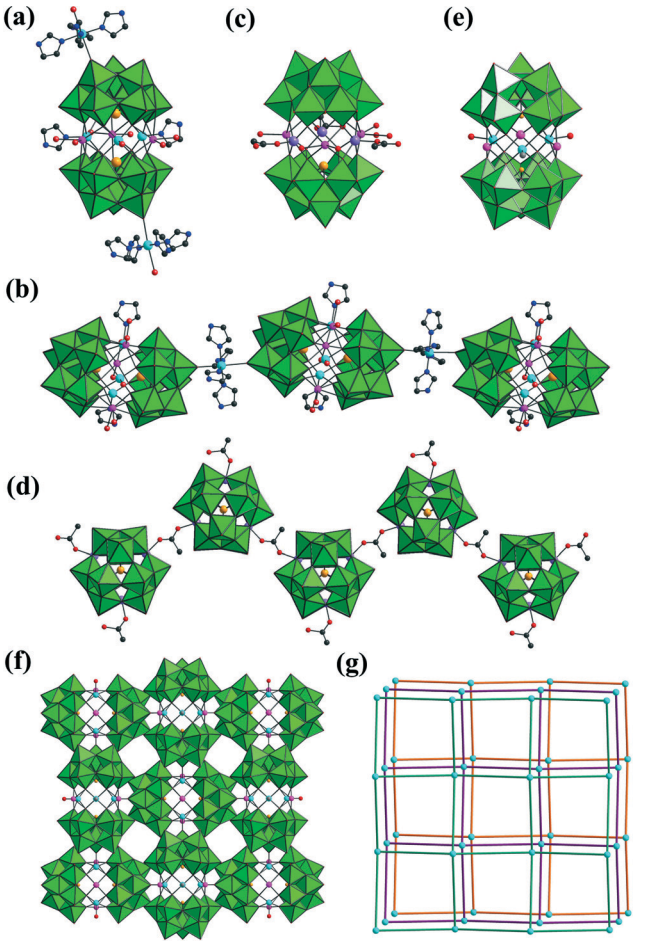

Fig. 3 (a and b) View of the structural unit and the 1-D chain of $[\{Cu(im)_4\}\{Na(H_2O)_2\}_3\{Cu_3(im)_2(H_2O)\}(XW_9O_{33})_2]_{2n}$ [Cu: turquoise, C: gray-80%, N: blue]. (c and d) View of the structural unit and the 1-D chain of $[Na_3(H_2O)_6Mn_3(\mu\text{-}CH_3COO)_2(B\text{-}\alpha\text{-}SbW_9O_{33})_2]^{11-}$ [Mn: purple, C: gray-80%]. (e) View of $[Na_2Cu_4Cl(B\text{-}\alpha\text{-}SbW_9O_{33})_2]^{9-}$ [Cu: turquoise, Cl: gray-50%] [Cu: turquoise, C: gray-80%, N: blue]. (f and g) The 2-D network and the 2-D topology of $[Na_2Cu_4Cl(B\text{-}\alpha\text{-}SbW_9O_{33})_2]^{9-}$ [Cu: turquoise, Cl: gray-50%]. WO_6: bright green, Na: pink, O: red, X: light orange.

coordination of Cu^{2+} cations of the hexa-atomic ring, while the acetate ligands in $[Na_3(H_2O)_6Mn_3(\mu\text{-}CH_3COO)_2(B\text{-}\alpha\text{-}SbW_9O_{33})_2]^{11-}$ not only take part in the coordination of Mn^{2+} cations, but also have the bridging function in the creation of the beautiful 1-D sinusoidal chain (Fig. 3d). Furthermore, the magnetic behaviors of both $[\{Cu(im)_4\}\{Na(H_2O)_2\}_3\{Cu_3(im)_2(H_2O)\}(XW_9O_{33})_2]_{2n}$ (X = Bi^{III} and Sb^{III}) and $[Na_3(H_2O)_6Mn_3(\mu\text{-}CH_3COO)_2(B\text{-}\alpha\text{-}SbW_9O_{33})_2]^{11}$ indicate the dominant antiferromagnetic exchange interactions among the metal centers. Apart from the carboxylate-bridging 1-D chain PMGTMHD, Niu's group simultaneously addressed a $\{Na_2Cu_4\}$-ring sandwiched PMGTMHD $[Na_2Cu_4Cl(B\text{-}\alpha\text{-}SbW_9O_{33})_2]^{9-}$ (Fig. 3e), in which polyoxoanion building blocks were in conjunction with each other *via* Cu–O–W linkages to build up an attractive 2-D network structure (Fig. 3f and g).[26b] Moreover, similar infinitely extended 2-D networks based on hexa-nuclear sandwich-type heteropolyanions

were also reported by Kortz's group[26c] and Zhai's group.[26d] It should be noted that the hexa-metal $\{Na_2Cu_4\}$ central belt of $[Na_2Cu^{I}Cu^{II}(OH_2)Cu_2{}^{II}(B\text{-}\alpha\text{-}SbW_9O_{33})_2]^{9-}$ reported by Zhai's group contained mixed-valence Cu^{+}/Cu^{2+} ions, which made it exhibit excellent catalytic activity towards the electron transfer reaction of ferricyanide to ferrocyanide by thiosulphate in an aqueous medium. This study will give chemists a great impetus to exploit potential applications of POT-based materials.[26d]

3 The progress with PTMTMHDs

To date, abundant PTMTMHDs have been acquired.[27] Generally speaking, most PTMTMHDs are sandwich-type structures that consist of two trivacant Keggin ($[XW_9O_{33-34}]^{n-}$, X = $As^{III/V}$, Ge^{IV}, Si^{IV}, P^{V}, and Sb^{III}) or Dawson ($[X_2W_{15}O_{56}]^{12-}$, X = P^{V} and As^{V}) segments anchoring a TM core.[27a–i] In 2001, Hill *et al.* reported the sandwich-type PMGTMHD $[Fe^{III}{}_2(NaOH_2)_2(P_2W_{15}O_{56})_2]^{16-}$, in which two Fe^{3+} ions are located at two exterior positions and two Na^{+} ions occupy two interior positions in the sandwich belt.[24g] It turned out to be an excellent candidate for the design of PTMTMHDs by introducing extraneous TM ions to replace the Na^{+} ions in the sandwich belt, which is in good agreement with the fact that Na^{+} ions in the sandwiched belt are weakly bonded to POT fragments and are labile for substitution. Therefore, the multistep substitution method in which one or two temporally "plugged" alkali-metal ions in prefabricated sandwich-type PMGTMHDs are replaced by another TM ions is very popular method to prepare PTMTMHDs. Hill, Thouvenot, Mbomekallé *et al.* made some progress in this respect.[27a–h] For example, the reaction of one or two Fe^{3+} ions stoichiometrically with $[Na_2(H_2O)_2Ni_2(As_2W_{15}O_{56})_2]^{18-}$ led to two new mixed-metal POTs, namely, $[Fe(OH_2)Ni(OH_2)Ni_2(As_2W_{15}O_{56})_2]^{15-}$ (Fig. 4a) and $[Fe_2(H_2O)_2Ni_2(As_2W_{15}O_{56})_2]^{14-}$, whereas the incorporation of Ni^{2+} ions to $[Na_2(H_2O)_2Fe_2(As_2W_{15}O_{56})_2]^{16-}$ led to another new mixed-metal complex $[Ni_2(H_2O)_2Fe_2(As_2W_{15}O_{56})_2]^{14-}$,[27a] which illustrates that the structures and properties of PTMTMHDs can be finely tuned by changing the spatial distribution of metal centers under controlled experimental conditions. However, the introduction of excess Co^{2+} or Cu^{2+} ions to the $[Fe^{III}{}_2(NaOH_2)_2(P_2W_{15}O_{56})_2]^{16-}$ aqueous system resulted in a new type of PTMTMHD $[M^{II}Fe^{III}{}_2(P_2W_{15}O_{56})(P_2M^{II}{}_2W_{13}O_{52})]^{16-}$ (M = Co^{2+}, Cu^{2+}) (Fig. 4b),[27h] whose structure consisted of a classic trivacant $\{P_2W_{15}\}$ unit and a di-substituted trivacant $\{P_2M^{II}{}_2W_{13}\}$ unit, sandwiching a $\{Fe^{III}{}_2M^{II}\}$ central unit. The catalytic evaluation demonstrates that their TBA salts are stable and effective catalysts for the oxidation of alkenes with participation of H_2O_2.[27h] Besides, two intriguing TM–Ru-substituted PTMTMHDs $[\{Ru^{IV}{}_4O_6(H_2O)_9\}_2\{Fe(H_2O)_2\}_2\{\beta\text{-}TeW_9O_{33}\}_2H]^{-}$ (Fig. 4c) and $[\{B\text{-}\alpha\text{-}AsW_9O_{34}\}\{B\text{-}\beta\text{-}AsW_8O_{31}\}\{Zn_4(OH)_2(H_2O)_2\}\{(RuC_6H_6)_3\}]^{6-}$ (Fig. 4d) were reported by the Kortz group.[27i,j] The former was isolated by the reaction of $(NH_4)_2[RuCl_6]$ with the classic tetra-TM-sandwiched $[Fe_4(H_2O)_{10}(\beta\text{-}TeW_9O_{33})_2]^{4-}$ in an aqueous acidic medium (pH 1.5), which displays that two adamantane-like tetra-Ru^{IV} units $[Ru_4O_6(H_2O)_9]^{4+}$ substituted two external Fe^{3+} ions of the precursor $[Fe_4(H_2O)_{10}(\beta\text{-}TeW_9O_{33})_2]^{4-}$,[27i] whereas the latter was accomplished by reacting $[RuC_6H_6Cl_2]_2$ with the trivacant precursor $[B\text{-}\alpha\text{-}AsW_9O_{34}]^{9-}$ and $ZnAc_2$ in a 3 : 4 : 8 ratio in a buffer solution (pH = 6.0), and exhibits a rhombic quadrimeric cluster $\{Zn_4O_{12}(OH)_2(H_2O)_2\}$ anchored between two different Keggin units $\{B\text{-}\alpha\text{-}AsW_9O_{34}\}$ and $\{B\text{-}\beta\text{-}AsW_8O_{31}\}$ to produce an asymmetric sandwiched fragment $[\{B\text{-}\alpha\text{-}AsW_9O_{34}\}\{B\text{-}\beta\text{-}AsW_8O_{31}\}\{Zn_4(OH)_2(H_2O)_2\}]^{12-}$, which is further coordinated by three $\{RuC_6H_6\}$ units through three Ru–O–W, four Ru–O–W(Zn) and two Ru–O–Zn bonds forming an unprecedented hybrid polyanion $[\{B\text{-}\alpha\text{-}AsW_9O_{34}\}\{B\text{-}\beta\text{-}AsW_8O_{31}\}\{Zn_4(OH)_2(H_2O)_2\}\{(RuC_6H_6)_3\}]^{6-}$, and it represents the first PTMTMHD comprised of a TM-sandwiched POT unit with organoruthenium groups.[27j] Subsequently, a series of analogical complexes $[\{B\text{-}\alpha\text{-}AsW_9O_{33}(OH)\}\{B\text{-}\beta\text{-}AsW_8O_{30}(OH)\}\{M_4(OH)_2(H_2O)_2\}\{(RuC_6H_6)_3\}]^{6-}$ (M = Ni^{2+}, Zn^{2+}, Cu^{2+}, Mn^{2+}, and Co^{2+}) were achieved by Bi's group.[27k] Furthermore, Mizuno *et al.* put forward a single-step synthetic strategy and obtained two M_2Zn_2-sandwiched silicotungstates $[\{M(OH_2)_2(\mu_3\text{-}OH)\}_2Zn(OH_2)_2\}_2\{\gamma\text{-}HSiW_{10}O_{36}\}_2]^{8-}$ (M = Co^{2+} and Ni^{2+}) (Fig. 4e).[27l] To the best of our knowledge, this is the first example of 3d–3d′ heterometallic substituted POTs by a single-step synthesis in an organic solvent. Interestingly, the assembly of these rigid $[\{M(OH_2)_2(\mu_3\text{-}OH)\}_2Zn(OH_2)_2\}_2\{\gamma\text{-}HSiW_{10}O_{36}\}_2]^{8-}$ anions with flexible TBA cations engenders porous ionic crystals that represent the largest pore and void sizes of POM-containing ionic crystals.[27l] This finding exhibits that the evolution of the synthetic approach from the conventional aqueous solution to the organic solvent system

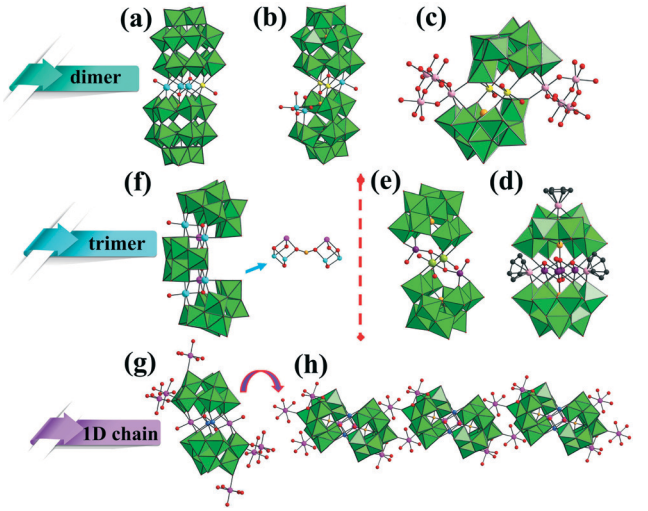

Fig. 4 (a) View of $[Fe(OH_2)Ni(OH_2)Ni_2(As_2W_{15}O_{56})_2]^{15-}$ [Fe: yellow and Ni: turquoise]. (b) View of $[TM^{II}Fe^{III}{}_2(P_2W_{15}O_{56})(P_2TM^{II}{}_2W_{13}O_{52})]^{16-}$ [Fe: yellow and TM: turquiose]. (c) View of $[\{Ru^{IV}{}_4O_6(H_2O)_9\}_2\{Fe(H_2O)_2\}_2\{\beta\text{-}TeW_9O_{33}\}_2H]^{-}$ [Ru: rose and Fe: yellow]. (d) View of $[\{B\text{-}\alpha\text{-}AsW_9O_{34}\}\{B\text{-}\beta\text{-}AsW_8O_{31}\}\{Zn_4(OH)_2(H_2O)_2\}\{(RuC_6H_6)_3\}]^{6-}$ [Ru: rose and Zn: violet]. (e) View of $[\{Co(OH_2)_2(\mu_3\text{-}OH)\}_2\ Zn(OH_2)_2\}_2\{\gamma\text{-}HSiW_{10}O_{36}\}_2]^{8-}$ [Co: lime and Zn: violet]. (f) Views of $[Ni_4Mn_2P_3W_{24}\ O_{94}(H_2O)_2]^{17-}$ and the alignment of its metal core. [Ni: turquoise, Mn: pink, and P: light orange]. (g and h) The structural unit and the 1-D linear chain of $[Mn_4(H_2O)_{18}W\ ZnMn_2(H_2O)_2(ZnW_9O_{34})_2]^{4-}$ [Mn: pink and WZn: light blue]. WO_6: bright green, O: red, X: light orange.

will lead to novel POM-based materials, accompanied with interesting structures and neoteric properties.

Trimeric hexanuclear POTs constructed from two $\{XW_9O_{34}\}$ fragments and one $\{XW_6O_{26}\}$ fragment linked by two trimeric TM clusters are always described as banana-shaped, C-shaped or V-shaped structures. However, few such PTMTMHDs have been reported.[28] When Kortz's group continued to explore the multistep substitution method with the motivation of substituting Na^+ ions in $[Ni_3Na(H_2O)_2(PW_9O_{34})_2]^{11-}$ by redox-active Mn(II) ions, unexpectedly, they discovered a neoretic banana-shaped PTMTMHD $[Ni_4Mn_2P_3W_{24}O_{94}(H_2O)_2]^{17-}$ (Fig. 4f),[28] in which two Mn^{2+} ions and four Ni^{2+} ions could not be distinguished by X-ray diffraction, but the combination of elemental analysis, electrochemistry and magnetism determined the formula. However, the exact distribution of six TM ions among two M_3O_{13} triads is a complicated problem. The experimental evidence merely show that each M_3O_{13} triad comprises one Mn^{2+} ion and two Ni^{2+} ions and the specific position of the Mn^{2+} ion can hardly be assigned to the M_3O_{13} triad (Fig. 4f shows one possible structural form). In addition, recently, a 1-D PTMTMHD $[Mn_4(H_2O)_{18}WZnMn_2(H_2O)_2(ZnW_9O_{34})_2]^{4-}$ (Fig. 4g) was obtained by Wu's group, in which each $[WZnMn_2(H_2O)_2(ZnW_9O_{34})_2]^{12-}$ unit is composed of a {MnWZnMn} ring belt sandwiched by two $\{ZnW_9O_{34}\}$ units where the two internal vacant sites are simultaneously occupied by 50% W and 50% Zn elements and two external positions are located by two Mn ions. Adjacent $[WZnMn_2(H_2O)_2(ZnW_9O_{34})_2]^{12-}$ units are ligated by the bridging Mn^{2+} cations to construct a 1-D linear chain (Fig. 4h).[29] Surprisingly, under the induction effect of Co^{2+} or Cu^{2+} ions, This PTMTMHD can undergo 1-D to 3-D single-crystal-to-single-crystal structural transformation into two novel POTs with four types of TM components $\{[M_2(H_2O)_6][Mn_4(H_2O)_{16}][WZn(Mn(H_2O))_2(ZnW_9O_{34})_2]\}\cdot 10H_2O$ [M = Co^{2+}, Cu^{2+}], which display good catalytic activity for the oxidative aromatization of Hantzsch 1,4-dihydropyridines.[29]

4 The progress in PRETMHDs

In the past decade, many inorganic and inorganic–organic hybrid PRETMHDs with monomeric to polymeric structures have been discovered by the conventional aqueous method or hydrothermal treatment. In 2008, Kögerler *et al.* first demonstrated a straightforward approach to synthesize divacant Dawson monomeric PRETMHD $[\{\alpha\text{-}P_2W^{VI}{}_{16}O_{57}(OH)_2\}\{Ce^{IV}Mn^{IV}{}_6O_9(OOCCH_3)_8\}]^{8-}$ (Fig. 5a) with a $\{Ce^{IV}Mn^{IV}{}_6O_9(OOCCH_3)_8\}$ core (Fig. 5b) by treating the prefabricated heterometallic complex $[Ce^{IV}Mn^{IV}{}_6O_9(OOCCH_3)_9(NO_3)(H_2O)_2]$ (ref. 30) with the trivacant Dawson polyoxoanion $[\alpha\text{-}P_2W_{16}O_{56}]^{12-}$ in the CH_3COOH–H_2O solution in the presence of $[(CH_3)_2NH_2]\cdot HCl$.[18a] Its magnetic behavior manifests antiferromagnetic coupling interactions between the S = 3/2 Mn^{4+} center with a singlet ground state.

A library of inorganic dimers or dimers decorated by organic ligands have been reported. In 2010, by the reaction of Ce^{4+} ions with the tetra-Mn^{II}-substituted $[Mn^{II}{}_4(H_2O)_2(B\text{-}\alpha\text{-}GeW_9O_{34})_2]^{12-}$ in water with the addition of Cs^+ ions, Reinoso *et al.* acquired a dimeric weak ferromagnetic PRETMHD $[\{Ce^{III}(H_2O)_2\}_2Mn^{III}{}_2(B\text{-}\alpha\text{-}GeW_9O_{34})_2]^{8-}$ (Fig. 6a), which can be described as two outer $[Mn(H_2O)]^{2+}$ groups being substituted by two $[Ce(H_2O)_2]^{3+}$ groups, creating an unprecedented rhomb-like $\{Ce_2Mn_2O_{20}\}$ cluster.[19a] Interestingly, the formation of $[\{Ce^{III}(H_2O)_2\}_2Mn^{III}{}_2(B\text{-}\alpha\text{-}GeW_9O_{34})_2]^{8-}$ may undergo the removal of the outer $[Mn(H_2O)]^{2+}$ groups, accompanying the oxidation of Mn^{2+} ions to Mn^{3+} ions exerted by Ce^{4+} ions. Very recently, Zhao *et al.* discovered a group of novel purely inorganic Fe^{III}–RE^{III} heterometallic tungstoantimonates $[RE(H_2O)_7]_2[Fe_4(H_2O)_{10}][B\text{-}\beta\text{-}SbW_9O_{33}]_2\cdot 22H_2O$ (RE = Tb^{3+}, Dy^{3+}, Lu^{3+}, Y^{3+}) (Fig. 6b) by the reaction of $[B\text{-}\alpha\text{-}SbW_9O_{33}]^{9-}$, Fe^{3+} and RE^{3+} ions in a conventional aqueous solution, which are composed of a tetra-Fe^{III}-substituted sandwiched unit $[Fe_4(H_2O)_{10}(B\text{-}\beta\text{-}SbW_9O_{33})]^{6-}$ decorated by two $[RE(H_2O)_8]^{3+}$ cations.[31] To the best of our knowledge, they represent the first purely inorganic PRETMHDs containing tungstoantimonate fragments. Subsequently, Zhang *et al.* found another new tungstoantimonate-based PRETMHD $[K_2Dy_2Cu_2(H_2O)_8(SbW_9O_{33})_2]^{6-}$ (Fig. 6c) from the reaction of the preformed large precursor $[Na_2Sb_8W_{36}O_{132}(H_2O)_4]^{22-}$ with Cu^{2+} and Dy^{3+} ions.[32] This 3d–4f heterometallic sandwiched polyoxoanion was combined with two extra 4p cations to obtain a novel POT including a ring-like 3d–4f–4p cluster. Furthermore, the electrochemical study indicated that this compound shows the electrocatalytic activity for the reduction of NO_2^- and O_2, and a direct 4-electron reduction process from O_2 to H_2O has been observed in an aqueous solution for this compound. In contrast, dimeric PRETMHDs with tetravacant POT segments are relatively rare.[3c,20a] In 2013, Wang's group prepared a novel PRETMHD $[\{Dy^{III}Mn^{III}{}_4(\mu_3\text{-}O)_2(\mu_2\text{-}OH)_2(H_2O)(CO_3)(\beta\text{-}SiW_8O_{31})_2]^{13-}$ (Fig. 6d) by the mixture of divacant $[\gamma\text{-}SiW_{10}O_{38}]^{8-}$, Mn^{2+}, Dy^{3+} and CO_3^{2-} ions in an aqueous solution, which is composed of two tetravacant $\{\beta\text{-}SiW_8O_{31}\}$ units encapsulating a pentanuclear $\{DyMn_4\}$ moiety with one anchoring CO_3^{2-} anion (Fig. 6e).[3c] Magnetic measurements indicate a SMM-like (single molecule magnet) feature in the heterometallic cluster.[3c] It is worth mentioning that it not only represents the first appended heterometallic cubane sandwiched by pure inorganic POT ligands, but also delegates the first tetravacant Keggin PRETMHD. Later, isostructural species were also isolated by them.[20a] Except for purely inorganic dimeric PRETMHDs, inorganic–organic

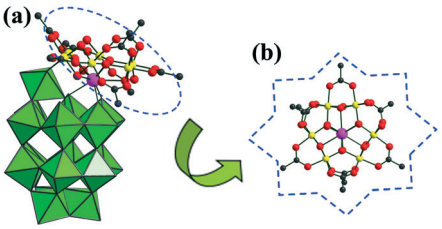

Fig. 5 (a) View of $[\{\alpha\text{-}P_2W^{VI}{}_{16}O_{57}(OH)_2\}\{Ce^{IV}Mn^{IV}{}_6O_9(OOCCH_3)_8\}]^{8-}$. (b) View of $\{Ce^{IV}Mn^{IV}{}_6O_9(OOCCH_3)_8\}$. WO_6: bright green, Ce: pink, Mn: yellow, O: red, C: gray-80%, N: blue, X: light orange.

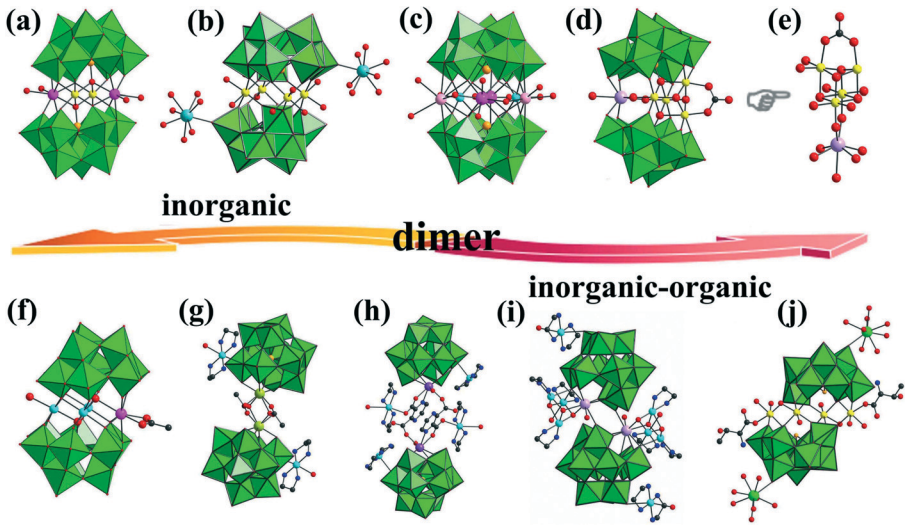

Fig. 6 (a) View of $[\{Ce^{III}(H_2O)_2\}_2Mn^{III}_2(B\text{-}\alpha\text{-}GeW_9O_{34})_2]^{8-}$ [Ce: pink and Mn: yellow]. (b) View of $[RE(H_2O)_7]_2[Fe_4(H_2O)_{10}][B\text{-}\beta\text{-}SbW_9O_{33}]_2{\cdot}22H_2O$ [RE: aqua; Fe: yellow]. (c) View of $[\{K_2Dy_2Cu_2(H_2O)_8(SbW_9O_{33})_2\}]^{6-}$ [Dy: purple, Cu: turquoise, and K: rose]. (d) and (e) View of $[\{Dy^{III}Mn^{III}_4(\mu_3\text{-}O)_2(\mu_2\text{-}OH)_2(H_2O)(CO_3)\}(\beta\text{-}SiW_8O_{31})_2]^{13-}$ and the heterometal {$DyMn_4$} moiety [Dy: lavender and Mn: yellow]. (f) $[\{Ce^{IV}(CH_3COO)\}Cu^{II}_3(H_2O)(B\text{-}\alpha\text{-}GeW_9O_{34})_2]^{11-}$ [Ce: pink and Cu: turquoise]. (g) View of $[(\alpha\text{-}XW_{11}O_{39})RE(H_2O)(\eta^2,\mu\text{-}1,1)\text{-}CH_3COO]_2^{10/12-}$ [Cu: turquoise and Sm; lime]. (h) View of $\{[Cu(en)_2][Cu(en)_2(H_2O)][(\alpha\text{-}SiW_{11}O_{39})RE(H_2O)(pzda)]\}_2^{6-}$ [Cu: turquoise and RE: purple], (i) view of $\{[Cu_3RE(en)_3(OH)_3(H_2O)_2](\alpha\text{-}GeW_{11}O_{39})\}_2^{4-}$ [Cu: turquoise and Eu: lavender]. (j) View of $[RE(H_2O)_8]_2[Fe_4(H_2O)_8(thr)_2][B\text{-}\beta\text{-}SbW_9O_{33}]_2{\cdot}22H_2O$ [RE: bright green and Fe: yellow]. WO_6: bright green, O: red, C: gray-80%, N: blue and X: light orange.

dimeric PRETMHDs comprising O- and N-containing organic ligands or aminoacid ligands have also been reported.[19b,c,20b,d,34] For example, Reinoso's group and Yang's group respectively addressed two types of dimeric PRETMHDs based on acetate ligands $[\{Ce^{IV}(CH_3COO)\}Cu_3(H_2O)(B\text{-}\alpha\text{-}GeW_9O_{34})_2]^{11-}$ (Fig. 6f)[19c] and $[(\alpha\text{-}XW_{11}O_{39})RE(H_2O)(\eta^2,\mu\text{-}1,1)\text{-}CH_3COO]_2^{10/12-}$ [(X, RE) = (Si^{IV}, Tb^{3+}), (P^V, Sm^{3+})] (Fig. 6g).[20c] The distinctions between them are as follows: (i) from the viewpoint of synthetic strategy, the former was achieved *via* the step-by-step method in an aqueous solution, while the latter was accomplished by the one-pot self-assembly reaction under hydrothermal conditions; (ii) from the structural point of view, the former can be described as one outer $[Cu(H_2O)]^{2+}$ ion in the precursor was substituted by an extraneous $\{Ce(CH_3COO)\}^{3+}$ group, whereas the latter is formed when two 1 : 1-type mono-RE-substituted Keggin POT moieties are bridged by two acetate ligands. In addition, using the saturated $[SiW_{12}O_{40}]^{4-}$ precursor and RE ions as the starting material in the presence of mixed flexible en and rigid pzda ligands (pzda = pyrazine-2,3-dicarboxylate), Niu and co-workers hydrothermally prepared a family of novel dimeric PRETMHDs with mixed organic ligands $\{[Cu(en)_2][Cu(en)_2(H_2O)][(\alpha\text{-}SiW_{11}O_{39})\text{-}RE(H_2O)(pzda)]\}_2^{6-}$ (RE = Y^{3+}, Dy^{3+}, Yb^{3+}, Lu^{3+}) (Fig. 6h), in which two mono-RE-substituted $[RE(\alpha\text{-}SiW_{11}O_{39})]^{5-}$ segments were connected together by pzda ligands and $[Cu(en)_2]^{2+}$ and $[Cu(en)_2(H_2O)]^{2+}$ cations as pendants link to the periphery of them.[20b] Notably, Zhao *et al.* obtained three interesting dimeric tungstogermanate-based PRETMHDs $\{[Cu_3RE(en)_3\text{-}(OH)_3(H_2O)_2](\alpha\text{-}GeW_{11}O_{39})\}_2^{4-}$ (RE = Eu^{3+}, Tb^{3+}, Dy^{3+}) (Fig. 6i), which are built by two {Cu_3LnO_4} cubane anchored mono-vacant $[\alpha\text{-}GeW_{11}O_{39}]^{8-}$ fragments through two W–O–Ln–O–W linkers.[19b] The investigations on of their magnetic properties illustrates that there are antiferromagnetic coupling interactions within {Cu_3EuO_4} cubane units, whereas the weak ferromagnetic interactions exist in the {Cu_3Tb/DyO_4} cubane units. The results are consistent with the previous conclusion made by Kahn *et al.* and Costes *et al.* that the Cu^{II}–RE^{III} interactions are antiferromagnetic when RE = Ce^{3+}, Nd^{3+}, Sm^{3+}, Tm^{3+}, and Yb^{3+}, while the Cu–RE interactions are ferromagnetic when RE = Gd^{3+}, Tb^{3+}, Dy^{3+}, Ho^{3+}, and Er^{3+}, and as for Cu^{II}–Pr^{III} and Cu^{II}–Eu^{III} complexes, the Pr^{3+} and Eu^{3+} ions are nonmagnetic at low temperatures.[33] Subsequently, Zhao's group succeeded in making a class of threonine-decorated PRETMHDs $[RE(H_2O)_8]_2[Fe_4(H_2O)_8(thr)_2][B\text{-}\beta\text{-}SbW_9O_{33}]_2{\cdot}22H_2O$ (RE = Pr^{3+}, Nd^{3+}, Sm^{3+}, Eu^{3+}, Gd^{3+}, Dy^{3+}, and Lu^{3+}; thr = threonine) (Fig. 6j),[34] each molecular structure of which comprises a $[Fe_4(H_2O)_8(thr)_2(B\text{-}\beta\text{-}SbW_9O_{33})]^{6-}$ anion with two supporting $[RE(H_2O)_8]^{3+}$ cations on both sides, delegating the first inorganic–organic hybrid Fe^{III}–RE^{III} heterometallic tungstoantimonates. In comparison with $[RE(H_2O)_7]_2[Fe_4(H_2O)_{10}][B\text{-}\beta\text{-}SbW_9O_{33}]_2{\cdot}22H_2O$ (RE = Tb^{3+}, Dy^{3+}, Lu^{3+}, Y^{3+}) mentioned above,[31] apart from the difference that two water ligands in the classic $[Fe_4(H_2O)_{10}(B\text{-}\beta\text{-}SbW_9O_{33})_2]^{6-}$ have been substituted by two thr ligands, it is clearly seen that the coordination positions of two supporting $[RE(H_2O)_8]^{3+}$ cations are away from the sandwich belt of the polyoxoanion $[Fe_4(H_2O)_8(thr)_2(B\text{-}\beta\text{-}SbW_9O_{33})]^{6-}$. The fluorescence spectrum of $[Eu(H_2O)_8]_2[Fe_4(H_2O)_8(thr)_2][B\text{-}\beta\text{-}SbW_9O_{33}]_2{\cdot}22H_2O$ under excitation at 310 nm shows five characteristic emission peaks of Eu^{3+} ions associated with $^5D_0 \rightarrow {}^7F_J$ (J = 0, 1, 2, 3, 4) [$^5D_0 \rightarrow {}^7F_0$ (564 nm), $^5D_0 \rightarrow {}^7F_1$ (594 nm), $^5D_0 \rightarrow {}^7F_2$ (618 nm), $^5D_0 \rightarrow {}^7F_3$ (648 nm), and $^5D_0 \rightarrow {}^7F_4$ (700 nm)] transitions and the semilogarithmic plot of the luminescent decay curve can be indexed to the lifetime of 0.097 ms.[34] When thr was applied

to the arsenotungastate system under hydrothermal conditions, a series of thr-modified PRETMHDs based on arsenotungastates was obtained by them.[21b]

In 2008, Wang *et al.* synthesized a novel tungstoarsenate-based trimeric Keggin-type PRETMHD [K ⊂ {FeCe($AsW_{10}O_{38}$)-$(H_2O)_2$}$_3$]$^{14-}$ (Fig. 7a) in an acidic aqueous medium.[2a] This aggregate is made up of three dilacunary {α-$AsW_{10}O_{38}$} subunits linked by three {Fe–(μ_3-O)$_3$–Ce} heterometallic cluster forming an unusual cryptand-type trimer along with a K^+ ion encapsulated in its central cavity.[2a] In 2009, this group found another trimeric Dawson-type PRETMHD {[$Ce^{IV}_3Mn^{IV}_2O_6(CH_3COO)_6$-$(H_2O)_9$]$_2$($Mn^{III}_2P_2W_{16}O_{60}$)$_3$}$^{20-}$ (Fig. 7b) by deliberately introducing a hexavacant precursor [$H_2P_2W_{12}O_{48}$]$^{12-}$ into the CH_3COOH–CH_3COONa system including Ce^{4+} and Mn^{2+} ions, which consisted of an extraordinary triple-Dawson-type polyoxoanion [$Mn^{III}_2P_2W_{16}O_{60}$]$_3^{24-}$ and two 3d–4f heterometallic bipyramid-like clusters [$Ce^{IV}_3Mn^{IV}_2O_6(CH_3COO)_6(H_2O)_9$]$^{2+}$.[3b] Fang *et al.* used pre-prepared [$Mn^{III}_8Mn^{IV}_4O_{12}(CH_3$-$COO)_{16}(H_2O)_4$] (ref. 35) and [$CeMn_6O_9(CH_3COO)_9(NO_3)(H_2O)_2$] (ref. 30) clusters as Mn^{3+}/Mn^{4+} sources to react with [A-β-SiW_9O_{34}]$^{10-}$ in the CH_3COOH–CH_3COONa buffer and made an unprecedented tetrameric aggregate {Na_2[(A-β-SiW_9O_{34})$_2$ $Ce^{IV}_4O_2(CH_3COO)_2$][(A-β-SiW_9O_{34})$Mn^{III}_3Mn^{IV}O_3(CH_3$-$COO)_3$]$_2$}$^{20-}$ (Fig. 7c) exhibiting SMM behavior, which is constructed from a 1 : 2 molar co-crystallization of the diamagnetic Ce_4-sandwiched [(A-β-SiW_9O_{34})$_2Ce^{IV}_4O_2(CH_3$-$COO)_2$]$^{10-}$ subunit and the magnetic acetate-bridged [(A-β-SiW_9O_{34})$Mn^{III}_3Mn^{IV}O_3(CH_3COO)_3$]$^{6-}$ clusters linked by two Na^+ ions.[20d] Using the hydrothermal technology, another series of inorganic–organic hybrid tetrameric PRETMHDs {Cu(en)$_2$[RE(α-$GeW_{11}O_{39}$)$_2$]$_2$}$^{24-}$ (RE = La^{3+}, Pr^{3+}, Er^{3+}, and Eu^{3+}) (Fig. 7d) were synthesized by Zhao *et al.*, displaying that a [Cu(en)$_2$]$^{2+}$ bridge is in conjunction with two 1 : 2-type [RE(α-$GeW_{11}O_{39}$)$_2$]$^{13-}$ segments.[19b,d] Using large heteropolyanions such as cryptate [$NaAs_4W_{40}O_{140}$]$^{27-}$ {As_4W_{40}} or ring [$H_7P_8W_{48}O_{184}$]$^{33-}$ {P_8W_{48}} as precursors to react with TM and RE mixed ions is also an effective strategy to synthesize PRETMHDs on account that they can incorporate more TM or RE ions into their skeleton, forming unique aggregates. Xue and co-workers discovered the first series of PRETMHDs [RE$(H_2O)_5${Ni(H_2O)}$_2As_4W_{40}O_{140}$]$^{21-}$ (RE = Y^{3+}, Ce^{3+}, Pr^{3+}, Nd^{3+}, Sm^{3+}, Eu^{3+}, and Gd^{3+}) (Fig. 7e) by the reaction of {As_4W_{40}} with Ni^{2+} and RE^{3+} ions, which retains the cryptate structure featuring that two Ni^{2+} ions occupy the opposite two of four lacunary sites of the macrocyclic anion [$As_4W_{40}O_{140}$]$^{28-}$ and a RE^{3+} ion is located on the central cryptate site.[17] With a mixture of RE^{3+}, Fe^{3+} and {P_8W_{48}} in CH_3COOH–CH_3COOLi aqueous medium at pH = 4.0 in the presence of hydrogen peroxide, Kortz *et al.* isolated two giant horseshoe-shaped tetrameric PTMREHDs [$P_8W_{49}O_{189}Fe_{16}O_2$-$(OH)_{23}(H_2O)_9RE_4(H_2O)_{20}$]$^{11-}$ (RE = Eu^{3+}, Gd^{3+}) (Fig. 7f), comprising an open {P_8W_{49}} ring with a center [$Fe_{16}O_2(OH)_{23}(H_2O)_9$]$^{21+}$ core and four coordinated RE ions.[18c] Notably, the {P_8W_{49}} could be viewed as a rupture of the intact {P_8W_{48}} wheel with an extra W atom disordered 60 : 40 between equivalent cap positions at the two ends of the open {P_8W_{48}} wheel.[18c]

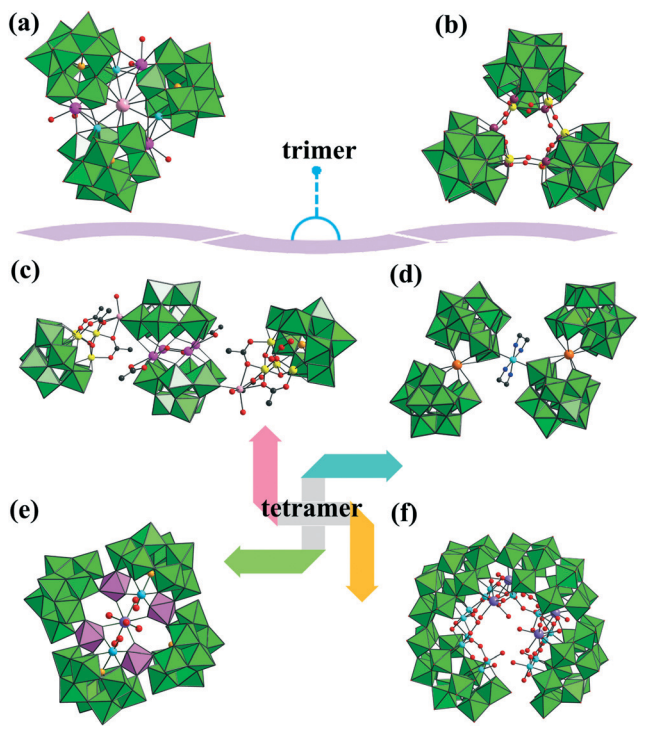

Fig. 7 (a) View of [K ⊂ {FeCe($AsW_{10}O_{38}$)(H_2O)$_2$}$_3$]$^{14-}$ [Ce: pink, Fe: turquoise, K: rose]. (b) View of {$Ce^{IV}_3Mn^{IV}_2O_6(CH_3COO)_6(H_2O)_9$]$_2$($Mn^{III}_2P_2W_{16}O_{60}$)$_3$}$^{20-}$ [Ce: pink: Mn: yellow]. (c) View of {Na_2[(A-β-SiW_9O_{34})$_2Ce^{IV}_4O_2(CH_3COO)_2$][(A-β-$SiW_9O_{34}$) $Mn^{III}_3Mn^{IV}O_3(CH_3COO)_3$]$_2$}$^{20-}$ [Ce: pink, Mn: yellow, Na: rose]. (d) View of {Cu(en)$_2$[La(α-$GeW_{11}O_{39}$)$_2$]$_2$}$^{24-}$ [Cu: turquoise; La: orange]. (e) View of [RE$(H_2O)_5${Ni(H_2O)}$_2As_4W_{40}O_{140}$]$^{21-}$ [RE: purple, Ni: sky blue, the bridging WO_6: rose purple]. (f) View of [$P_8W_{49}O_{189}Fe_{16}O_2(OH)_{23}(H_2O)_9RE_4(H_2O)_{20}$]$^{11-}$ [RE: purple, Fe: turquoise]. WO_6: bright green, O: red, C: gray-80%, N: blue, X: light orange.

Some much larger polymeric PRETMHDs were also reported.[3c,18a,b,19e–g,21a] In 2008, Kögerler *et al.* demonstrated that organic bridging ligands on Ce–Mn-carboxylate clusters can be partially substituted by polyoxoanions without altering the connectivity of the magnetic cluster core to synthesize novel PRETMHDs.[18a] Then, by the reaction of [α-$P_2W_{15}O_{56}$]$^{12-}$ with the high-oxidation-state heterometallic complex [$Ce^{IV}_3Mn^{IV}_2O_6(CH_3COO)_{7.5}(NO_3)_3$]·($CH_3COOH$)$_{0.5}$($H_2O$)$_2$ (ref. 30) in an aqueous solution in the presence of PO_4^{3-}, a ferromagnetic hexameric Dawson-type PRETMHD [{α-$P_2W_{15}O_{56}$}$_6${Ce_3-$Mn_2(\mu_3$-O)$_4(\mu_2$-OH)$_2$}$_3(\mu_2$-OH)$_2(H_2O)_2(PO_4)$]$^{47-}$ (Fig. 8a) was obtained, whose anion can be described as six trivacant Dawson [α-$P_2W_{15}O_{56}$]$^{12-}$ moieties, three [$Ce_3Mn_2O_6(OH)_2$]$^{6+}$ subunits and a central PO_4^{3-} group.[18b] It is noteworthy that an unexpected templating phosphate group subsequently directs these preconceived building blocks into a supercluster. In 2011, Wang *et al.* hydrothermally obtained two hexameric PRETMHDs [$K_7RE_6Fe_6(H_2O)_{12}(SiW_{10}O_{38})_6$]$^{29-}$ (RE = Dy^{3+}, Tb^{3+}) (Fig. 8b).[3a] In the skeleton, three [α-$SiW_{10}O_{38}$]$^{12-}$ subunits are connected by three heterometallic {Fe–(μ_3-O)$_3$–RE} linkers, giving rise to a trimeric cryptand-type subunit with a K^+ ion

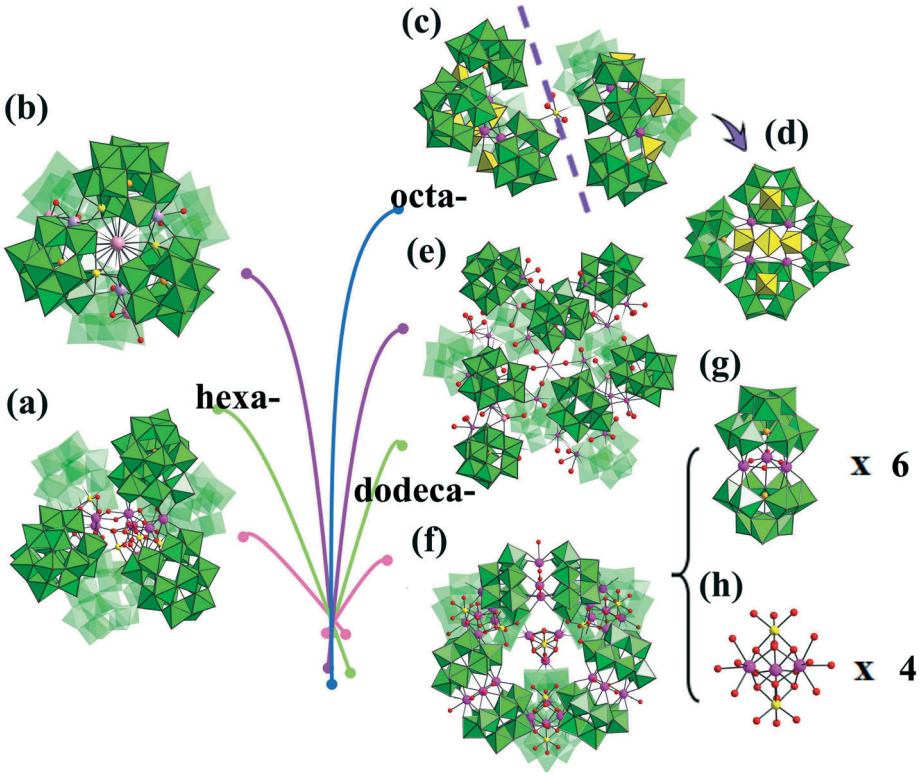

Fig. 8 (a) View of hexameric $[\{\alpha\text{-}P_2W_{15}O_{56}\}_6\{Ce_3Mn_2(\mu_3\text{-}O)_4(\mu_2\text{-}OH)_2\}_3(\mu_2\text{-}OH)_2(H_2O)_2(PO_4)]^{47-}$ [Ce: pink, Fe: yellow]. (b) View of hexameric $[K_7RE_6Fe_6(H_2O)_{12}(SiW_{10}O_{38})_6]^{29-}$ [RE: lavender, Fe: yellow, K: rose]. (c) View of octameric $\{Mn[Ce^{IV}_4As^{III}_4W_{41}O_{149}]_2\}^{46-}$ [Ce: pink, Mn: yellow, WO_5: yellow]. (d) View of cryptand-type $[Ce_4As_4W_{41}O_{149}]^{24-}$ subunit [Ce: pink, WO_5: yellow]. (e) View of dodecameric $[K \subset K_7Ce_{24}Ge_{12}W_{120}O_{456}(OH)_{12}(H_2O)_{64}]^{52-}$ [Ce: pink, K: rose]. (f) View of dodecameric $[\{(GeW_9O_{34})_2Dy_3(\mu\text{-}OH)_3(H_2O)\}_6\{Co_2Dy_3(\mu_3\text{-}OH)_6(OH_2)_6\}_4]^{56-}$ [Dy: purple, Co: yellow]. (g) View of sandwich-type $[(GeW_9O_{34})_2Dy_3(\mu\text{-}OH)_3(H_2O)]^{14-}$ [Dy: purple, Co: yellow]. (h) View of trigonal-bipyramidal heterometallic $[Co_2Dy_3(\mu_3\text{-}OH)_6(OH_2)_6]^{7+}$ [Dy: purple, Co: yellow]. WO_6: bright green, O: red, X: light orange. Some polyhedra are faded for clarity.

as the template, and then two trimeric cryptand-type subunit were further linked *via* five K^+ ions to generate the hexameric structural unit. The magnetic susceptibility measurements indicate the occurrence of antiferromagnetic interactions within the $\{Fe\text{–}(\mu_3\text{-}O)_3\text{–}RE\}$ clusters.[3a] Afterwards, Yang's group made a similar hexameric germanotungstate heterometallic species.[19e] In addition to these hexameric PRETMHDs, Wang *et al.* addressed an octameric aggregate $\{Mn[Ce^{IV}_4As^{III}_4W_{41}O_{149}]_2\}^{46-}$ (Fig. 8c) prepared by reacting a preformed RESP $\{[\{Ce_2O(H_2O)_5\}\{WO(H_2O)\}\{AsW_9O_{33}\}_2]_2\}^{32-}$ with Mn^{2+} ions, featuring two tetrameric cryptate $[Ce_4As_4W_{41}O_{149}]^{24-}$ (Fig. 8d) units bridged together by a $[Mn(H_2O)_4]^{2+}$ linker into a dimeric structure.[21a] In particular, the half unit $[Ce_4As_4W_{41}O_{149}]^{24-}$ can be viewed such that four $[B\text{-}\alpha\text{-}AsW_9O_{33}]^{9-}$ segments are connected by four Ce^{4+} and four W^{VI} centers, producing a new cryptate and another W^{VI} center that resides in the center of the cryptate.[21a] More interestingly, a crown-shape dodecameric complex $\{[Ni(H_2O)_6]_3[K \subset K_7Ce_{24}Ge_{12}W_{120}O_{456}(OH)_{12}(H_2O)_{64}]\}^{46-}$ (Fig. 8e) was separated by Reinoso *et al.* from the one-pot reaction in $CH_3COOH\text{–}CH_3COONa$ buffer, which can be seen as the outcome of the K^+-directed self-assembly of twelve *in situ* formed $[Ce_2GeW_{10}O_{38}]^{6-}$ subunits with three discrete $[Ni(H_2O)_6]^{2+}$ cations in the periphery.[19f] A close inspection of $[K \subset K_7Ce_{24}Ge_{12}W_{120}O_{456}(OH)_{12}(H_2O)_{64}]^{52-}$ showed that six $[\beta\text{-}Ce_2GeW_{10}O_{38}]^{6-}$ subunits are arranged alternately to form a hexameric $[K \subset \{[Ce(H_2O)_2]_2(\beta\text{-}GeW_{10}O_{38})\}_6]^{35-}$ crown-shape core, which is further reinforced by six outer $[\gamma\text{-}Ce_2GeW_{10}O_{38}]^{6-}$ units through O–Ce–O bridges to generate the unprecedented dodecameric aggregate.[19f] Very recently, Powell and collaborators isolated a giant tetrahedral heterometallic POT $[\{(GeW_9O_{34})_2Dy_3(\mu_2\text{-}OH)_3(H_2O)_2\}_6\{Co_2Dy_3(\mu_3\text{-}OH)_6(OH_2)_6\}_4]^{56-}$ (Fig. 8f) by a straightforward self-assembly procedure in an aqueous solution.[19g] In this structure, six sandwich-type building units $[(GeW_9O_{34})_2Dy_3(\mu\text{-}OH)_3(H_2O)]^{14-}$ (Fig. 8g) formed by two trilacunary $[A\text{-}\alpha\text{-}GeW_9O_{34}]^{10-}$ fragments connected by a planar triangular $[Dy_3(\mu\text{-}OH)_3(OH_2)]^{6+}$ group are combined together *via* four trigonal-bipyramidal heterometallic $[Co_2Dy_3(\mu_3\text{-}OH)_6(OH_2)_6]^{7+}$ (Fig. 8h) cationic clusters, producing a giant tetrahedral PRETMHD. To the best of our knowledge, it not only contains the largest number of RE ions of already reported POTs to date, but also synchronously represents the first example to two different TM–RE and RE cluster assemblies within a POT skeleton.[19g]

It is worth noting that POTs, as a sort of multidentate nucleophilic ligands to induce the formation of neoteric TM or RE clusters, are usually chosen as the starting materials that afford convenient platforms for modifying PRETMHDs while retaining their structural integrity and keeping their intrinsic properties, ultimately facilitating their implementation into

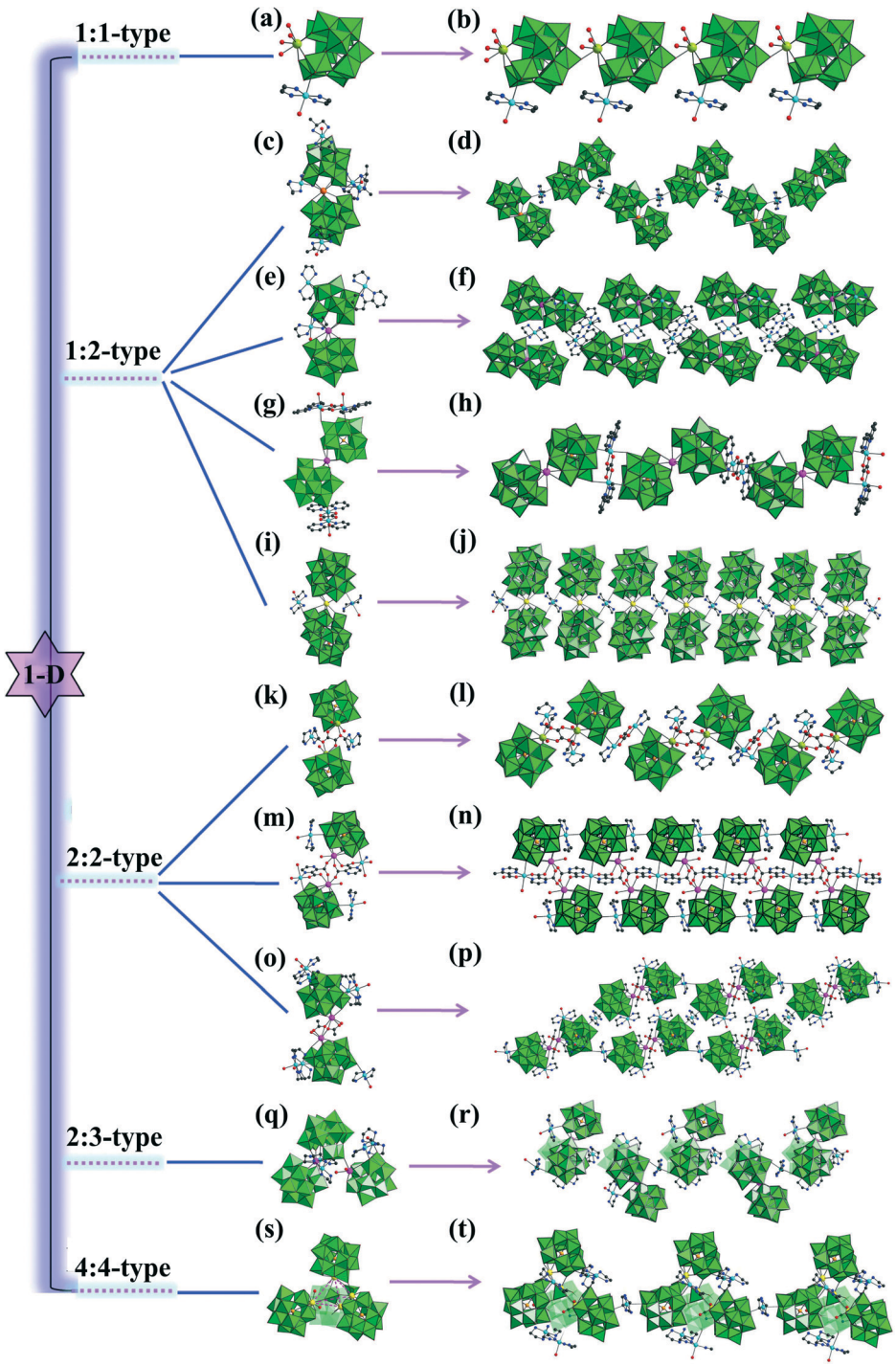

Fig. 9 (a and b) View of the structural unit and the 1-D liner chain of $[Cu(en)_2(H_2O)]_2[RE(\alpha\text{-}HXW_{11}O_{39})(H_2O)_3]\cdot 12H_2O$ [RE: lime]. (c and d) View of the structural unit and the 1-D zigzag chain of $[Cu(dap)(H_2O)_2]_{0.5}[Cu(dap)_2(H_2O)]_2[Cu(dap)_2]_3[RE(\alpha\text{-}AsW_{11}O_{39})_2]\cdot 3H_2O$ [RE: orange]. (e and f) View of the structural unit and the 1-D zigzag chain of $\{[Cu(en)_2]_{1.5}[Cu(en)(2,2'\text{-bpy})(H_2O)_n]RE[(\alpha\text{-}PW_{11}O_{39})_2]\}^{6-}$ [RE: pink]. (g and h) View of the structural unit and the 1-D zigzag chain of $[\{RE(PW_{11}O_{39})_2\}\{Cu_2(bpy)_2(\mu\text{-ox})\}]^{9-}$ [RE: pink]. (i and j) View of the structural unit and the 1-D chain of $[Cu(en)_2RE(\alpha_2\text{-}P_2W_{17}O_{61})_2]^{15-}$ [RE: yellow, Cu: turquoise]. (k and l) View of the structural unit and the 1-D chain architecture of $\{[Cu(en)_2][Tb(\alpha\text{-}PW_{11}O_{39})(H_2O)_2(ox)Cu(en)]\}_2^{2-}$ (Tb: lime). (m and n) View of the structural unit and the 1-D double chain of $\{[Cu(en)_2]_2[Cu(pzda)_2][(\alpha\text{-}H_2SiW_{11}O_{39})Ce(H_2O)]_2\}^{4-}$ [Ce: pink]. (o and p) View of the structural unit and the 1-D ladder-like chain of $[Cu(en)_2H_2O]_8[Cu(en)_2]_3[\{(\alpha\text{-}SiW_{11}O_{39})Ce(H_2O)(\eta^2,\mu\text{-}1,1\text{-}CH_3COO\}_4]^{2-}$ [RE: pink]. (q and r) View of the building unit and the 1-D chain motif of $\{[Cu(en)_2]_2[Dy_2(H_2O)_2(\alpha\text{-}GeW_{11}O_{39})_3]\}^{14-}$ [Dy: pink]. (s) View of the tetrahedral nanocluster unit $\{[(\alpha\text{-}GeW_{11}O_{39}RE)_2(\mu_3\text{-}WO_4)(\alpha\text{-}GeW_{11}O_{39}RE(H_2O))](\mu_4\text{-}WO_4)[\alpha\text{-}GeW_{11}O_{39}RE(H_2O)_2]\}^{24-}$ [RE: yellow]. (t) The 1-D chain architecture constructed from tetrahedral nanocluster units connected by $\{[Cu(en)_2]^{2+}$ bridges [RE: yellow]. Cu: turquoise, WO_6: bright green, O: red, C: gray-80%, N: blue, X: light orange. Some polyhedra are faded for clarity.

extended or high-dimensional architectures. The fact that most of the reported PRETMHDs are purely inorganic and isolated structures not only provides chemists great developing space and opportunity, but also motivates them to deeply explore the RE–TM–POT system in the hope of obtaining novel PRETMHDs with extended or high-dimensional structures. Thus, the hydrothermal method has become the major method to deal with this problem, and functional organic ligands can be deliberately introduced to the RE–TM–POT system. Several groups have made great contributions to the development of 1-D, 2-D and 3-D inorganic–organic hybrid PRETMHDs in the past several years.

Research results indicate that mono-RE-substituted POTs decorated by copper complexes serving as secondary building units widely exist in the structures of 1-D, 2-D and 3-D PRETMHDs. According to the ratio of RE cations and POT fragments, mono-RE-substituted POTs can be divided into five types: (i) the unusual 1 : 1-type monomeric structural unit with one RE ion grafting to the vacant site of $[\alpha\text{-}XW_{11}O_{39}]^{7/8-}$ (X = P^{V}, As^{V}, Si^{IV}, Ge^{IV}) fragment: $[Cu(en)_2(H_2O)]_2[RE(\alpha\text{-}XW_{11}O_{39})(H_2O)_3]\cdot 12H_2O$ (RE = Tb^{3+}, Eu^{3+}; X = Si^{IV}, Ge^{IV}) (Fig. 9a) prepared by Yang *et al.*[20c] Intriguingly, the structural units are connected with each other through W–O–RE–O–W bridges, constructing the rare 1-D chain arrangement (Fig. 9b).[20c] (ii) The common 1 : 2-type dimeric structural unit made up of one RE ion sandwiched by two monovacant Keggin-type or Dawson-type POT fragments: $[Cu(dap)(H_2O)_2]_{0.5}[Cu(dap)_2(H_2O)]_2$ $[Cu(dap)_2]_3[RE(\alpha\text{-}AsW_{11}O_{39})_2]\cdot 3H_2O$ (RE = Pr^{3+}, Eu^{3+}) (Fig. 9c)[21c] and $\{[Cu(en)_2]_{1.5}[Cu(en)(2,2'\text{-bpy})(H_2O)_n]RE[(\alpha\text{-}PW_{11}O_{39})_2]\}^{6-}$ [(RE, *n*) = (Ce^{3+}, 0), (Pr^{3+}, 1)] (Fig. 9e)[18d] made by Zhao *et al.* and Niu *et al.* and $[\{RE(PW_{11}O_{39})_2\}\{Cu_2(bpy)_2(\mu\text{-}ox)\}]^{9-}$ [(RE, *n*) = (La^{3+}/Pr^{3+}, 18), (Eu^{3+}, 16), (Gd^{3+}, 22), (Yb^{3+}, 19)] (Fig. 7g) made by Liu *et al.*,[18e] as well as $[Cu(en)_2RE(\alpha_2\text{-}P_2W_{17}O_{61})_2]^{15-}$ (RE = Tb^{3+}, Eu^{3+}, Sm^{3+}, and Ce^{3+}) (Fig. 9i) found by Yang *et al.*,[18f] in which adjacent $[RE(\alpha\text{-}XW_{11}O_{39})_2]^{11-}$ (X = As^{V}, P^{V}) or $[RE(\alpha_2\text{-}P_2W_{17}O_{61})_2]^{17-}$ units are combined to each other *via* copper-complex bridges, generating 1-D zigzag chains (Fig. 9d, f, h, j).[18d–f,21c] (iii) The novel 2 : 2-type dimeric structural unit built by two mono-RE-substituted POT fragments linked by two organic ligands: the ox-bridging $\{[Cu(en)_2][Tb(\alpha\text{-}PW_{11}O_{39})(H_2O)_2(ox)Cu(en)]\}_2^{2-}$ with the aesthetic 1-D chain alignment (Fig. 9k and l),[18g] the pzda-bridging $\{[Cu(en)_2]_2[Cu(pzda)_2][(\alpha\text{-}H_2SiW_{11}O_{39})Ce(H_2O)]_2\}^{4-}$ with the 1-D double chain fashion (Fig. 9m and n)[20b] and the CH_3COO-bridging $[Cu(en)_2H_2O]_8[Cu(en)_2]_3[\{(\alpha\text{-}SiW_{11}O_{39})Ce(H_2O)(\eta^2,\mu\text{-}1,1)\text{-}CH_3COO\}_4]^{2-}$ with the 1-D ladder-like structure (Fig. 9o and p)[20e] that were isolated by Yang *et al.*, Niu *et al.* and Su *et al.*, respectively. (iv) The scarce 2 : 3-type trimeric structural unit made by three monovacant Keggin-type POT fragments linked by two RE ions attained by Niu *et al.*: the 2 : 3-type mono-Dy-substituted Keggin germanotungstate $\{[Cu(en)_2]_2[Dy_2(H_2O)_2(\alpha\text{-}GeW_{11}O_{39})_3]\}^{14-}$ (Fig. 9q) exhibiting the 1-D extended architecture built by trimeric structural units and bridging $[Cu(en)_2]^{2+}$ cations (Fig. 9r).[19h] (v) The unique 4 : 4-type tetrameric structural unit constructed from four monovacant Keggin-type POT fragments bridged by four RE ions: tetrahedral POT-based nanocluster units $\{[(\alpha\text{-}GeW_{11}O_{39}RE)_2(\mu_3\text{-}WO_4)(\alpha\text{-}GeW_{11}O_{39}RE(H_2O))](\mu_4\text{-}WO_4)[\alpha\text{-}GeW_{11}O_{39}RE(H_2O)_2]\}^{24-}$ (RE = Gd^{3+}, Y^{3+}) (Fig. 9s) discovered by Zhao's group, in which mono-RE-substituted $[\alpha\text{-}GeW_{11}O_{39}RE(H_2O)_n]^{5-}$ (*n* = 0, 1, 2) fragments are fused together with the assistance of two WO_4^{2-} connectors to form a 4 : 4-type tetrameric RE core,[19i] and neighboring tetrahedral nanocluster units are alternately connected together with the participation of $[Cu(en)_2]^{2+}$ linkers, resulting in an unprecedented 1-D infinite chain architecture (Fig. 9t).[19i] In addition, other 1-D PRETMHDs including RE-substituted POTs were also made.[19j,20m,n]

It is generally known that sandwich-type TMSPs are usually of large volume and highly charged, which make them good candidates to react with RE ions, allowing for the formation of PRETMHDs. In 2010, Mialane *et al.* reported a tri-Cr^{III} sandwiched PRETMHD $[(\gamma\text{-}SiW_{10}O_{36})_2(Cr(OH)(H_2O))_3(La(H_2O)_7)_2]^{4-}$ (Fig. 10a) by the addition of excess La^{3+} ions to the pre-formed $[(\gamma\text{-}SiW_{10}O_{36})_2(Cr(OH)(H_2O))_3]^{10-}$ system.[20f] Intriguingly, dilacunary sandwiched $[(\gamma\text{-}SiW_{10}O_{36})_2(Cr(OH)(H_2O))_3]^{10-}$ subunits were bridged together by La^{3+} cations into a 1-D double-chain motif (Fig. 10b). Similarly, by treating Ce^{4+} ions with sandwich-type $[Mn_4Si_2W_{18}O_{68}(H_2O)_2]^{12-}$ in an acidic aqueous solution, an interesting tetra-Mn^{II}-sandwiched PRETMHD $[\{Ce(H_2O)_7\}_2Mn_4Si_2W_{18}O_{68}(H_2O)_2]^{6-}$ (Fig. 10c) was isolated by Wang *et al.*, which possessed a 1-D chiral ladder-like chain with a 2_1 screw axis that is constructed from trivacant Mn_4-sandwiched $[Mn_4Si_2W_{18}O_{68}(H_2O)_2]^{12-}$ units and $[Ce(H_2O)_7]^{3+}$ linkers (Fig. 10d).[20g] Apart from these 1D chains based on Keggin-type TMSPs, a new type of fascinating 1-D chain containing TM-substituted Dawson-type polyoxoanions were also made.[18h] By virtue of the multi-lacunary

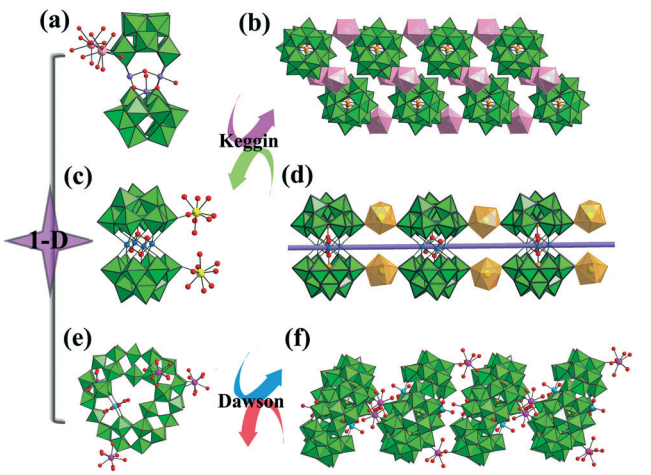

Fig. 10 (a and b) View of the structural unit and the 1-D double-chain motif of $[(\gamma\text{-}SiW_{10}O_{36})_2(Cr(OH)(H_2O))_3(La(H_2O)_7)_2]^{4-}$ [Cr: purple, La: rose, LaO_9: rose]. (c and d) View of the structural unit and the 1-D chain motif of $[\{Ce(H_2O)_7\}_2Mn_4Si_2W_{18}O_{68}(H_2O)_2]^{6-}$ [Ce: yellow, Mn: light blue, CeO_9: light orange]. (e and f) View of the structural unit and the 1-D chain of $[K_3 \subset \{GdCo(H_2O)_{11}\}_2\{P_6W_{41}O_{148}(H_2O)_7\}]^{13-}$ [Gd: pink, Co: sky blue]. WO_6: bright green, O: red, C: gray-80%, N: blue, X: light orange.

$[H_2P_2W_{12}O_{48}]^{12-}$ as the starting material, Wang *et al.* triumphantly isolated a di-Co^{II}-substituted complex $[K_3 \subset \{GdCo(H_2O)_{11}\}_2\{P_6W_{41}O_{148}(H_2O)_7\}]^{13-}$ (Fig. 10e) based on crown-shape unit $[\{WO(H_2O)\}_3(P_2W_{12}O_{48})_3]^{30-}$ that comprises three $[P_2W_{12}O_{48}]^{14-}$ moieties combined by three $\{WO(H_2O)\}$ linkers.[18h] More interestingly, neighboring Co-containing $[K_3 \subset \{Co(H_2O)_4\}_2\{P_6W_{41}O_{148}(H_2O)_7\}]^{20-}$ building blocks are in junction with each other by $[Gd(H_2O)_7]^{3+}$ connectors, giving rise to the captivating 1-D polymeric chain (Fig. 10f).[18h]

Niu's group and Zhao's group mainly concentrated on the reaction of POT precursors, Cu^{2+} and RE^{3+} cations in the participation of adapted exogenous ligands under hydrothermal environments and some 2-D Cu–RE heterometallic species based on 1 : 2-type RE-substituted POT units have been synthesized.[18d,20o,21c,d] For instance, starting from the [A-α-$HAsW_9O_{34}]^{8-}$ materials, Cu^{2+}, $RE^{3+/4+}$ and en, two types of inorganic–organic hybrid PRETMHDs $[Cu(en)_2(H_2O)]_4[Cu(en)_2]_2$-$[Cu(H_2O)_4]_{0.5}\{Cu(en)_2[H_2Ce^{IV}(\alpha\text{-}AsW_{11}O_{39})_2]_2\}\cdot 10H_2O$ (Fig. 11a) and $[Cu(en)_2(H_2O)][Cu(en)_2]_{1.5}[H_3RE(\alpha\text{-}AsW_{11}O_{39})_2]^{3-}$ (RE = Pr^{3+}, Nd^{3+}, Sm^{3+}, Eu^{3+}, Tb^{3+}) (Fig. 11b) were attained.[21c] In the former, each tetrameric unit $[Cu(H_2O)_4\{Cu(en)_2[H_2Ce(\alpha\text{-}AsW_{11}O_{39})_2]_2\}_2]^{26-}$ is connected with four adjacent tetrameric units through $[Cu(en)_2]^{2+}$ bridges, creating the unique 2-D sheet structure (Fig. 11c).[21c] Taking the tetrameric unit as a 4-connected node, the 2-D architecture established a 2-D (4,4)-topological network with the arrangement pattern of –AAA– (Fig. 11d).[21c] Unlike the former, the infrequent 2-D construction (Fig. 11e) of the latter is built from 1 : 2-type $[H_3RE(\alpha\text{-}AsW_{11}O_{39})_2]^{8-}$ building units by means of $[Cu(en)_2]^{2+}$ connectors, which possess a 3-connected (6,3)-topological network (Fig. 11f).[21c] In addition, the utilization of dap instead of en under the same conditions generates another type of PRETMHDs $[Cu(dap)_2]_{5.5}$ $[RE(\alpha\text{-}AsW_{11}O_{39})_2]\cdot xH_2O$ ((RE, x) = (Tb^{3+}, 6); (Dy^{3+}, 5)) (Fig. 11g).[21c] Interestingly, the 2-D sheet is also constructed from 1 : 2-type $[RE(\alpha\text{-}AsW_{11}O_{39})_2]^{11-}$ units and $[Cu(en)_2]^{2+}$ linkers (Fig. 11h), in which the $[RE(\alpha\text{-}AsW_{11}O_{39})_2]^{11-}$ subunits are looked on as 5-connected nodes and neighboring 2-D sheets are arranged in the mode of –AAA– (Fig. 11i).[21c] Furthermore, the photocatalytic measurements show that these PRETMHDs can, in some degree, inhibit the photodegradation of rhodamine-B.

In addition, Mialane *et al.* reported a 2-D PRETMHD based on 2 : 2-type di-RE-substituted POT units $\{[Cu(en)_2][(Cu(en)(OH))_3La(SiW_{11}O_{39})]\}_2\cdot 20H_2O$ (Fig. 12a).[20h] In the structure, neighboring dimeric $[(Cu(en)(OH))_3La(SiW_{11}O_{39})]_2^{4-}$ units are connected through La^{3+} cations into 1-D infinite chains and these 1-D chains are further bridged by $[Cu(en)_2]^{2+}$ groups, leading to a 2-D arrangement (Fig. 12b).[20h] In addition, Wang's group and Zhao's group further proved that tetra-TM sandwiched TMSPs are indeed active towards RE ions. In 2008, Wang's group reported a 2-D inorganic aggregate $\{Nd_2(H_2O)_{12}Cu_4(H_2O)_2(SiW_9O_{34})_2\}^{6-}$ (Fig. 12c) based on tetra-Cu-substituted $[Cu_4(H_2O)_2(SiW_9O_{34})_2]^{12-}$ units and Nd^{3+} linkers (Fig. 12d), representing the first 2-D purely inorganic sheet built from TM-sandwiched polyoxoanions and RE^{III} linkers.[20i] In 2015, Zhao *et al.* isolated a novel 2-D tungstoantimonate-based Fe^{III}–RE^{III} heterometallic POTs $[Pr(H_2O)_8][Pr(H_2O)_6][Fe_4(H_2O)_{10}][B\text{-}\beta\text{-}SbW_9O_{33}]_2\cdot 16H_2O$ (Fig. 12e).[31] It is interesting to note that the disordered Pr^{3+} cations act as bridges to link neighboring $[Fe_4(H_2O)_{10}(B\text{-}\beta\text{-}SbW_9O_{33})_2]^{6-}$ fragments, leading to the first 2-D extended framework in the family of tungstoantimonate-based PRETMHDs (Fig. 12f).[31] Apart from the 2-D sheets built with the aid of TM linkers or RE linkers, a giant 2-D aggregate $[K_3 \subset$

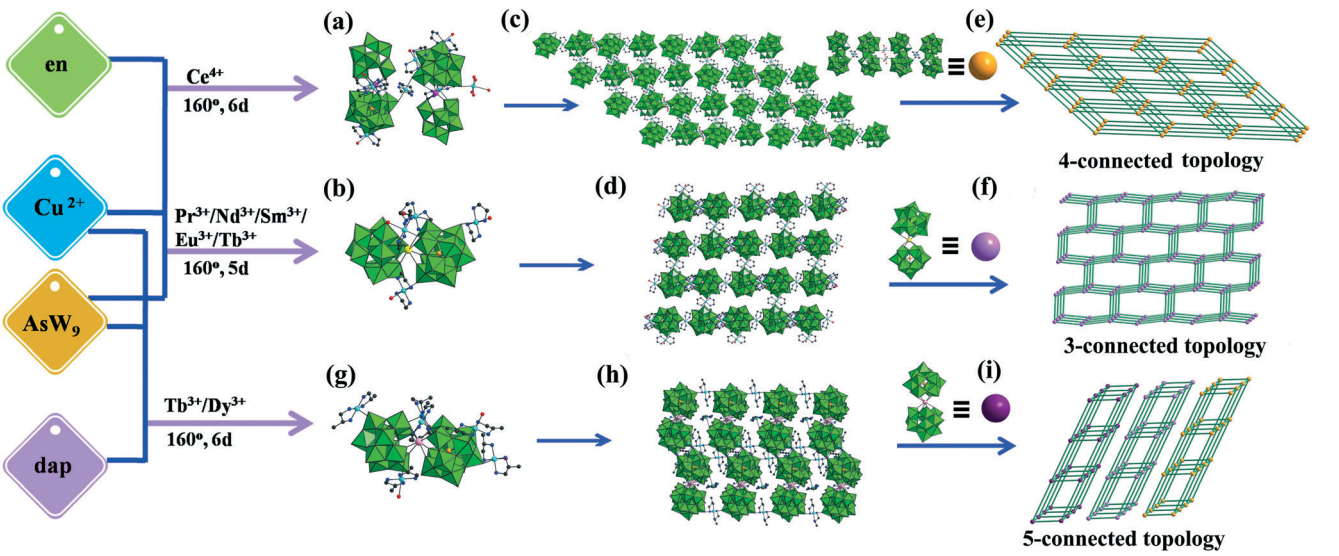

Fig. 11 (a, c and e) View of the structural unit, the 2-D sheet architecture and 2-D (4,4)-topological network of $[Cu(en)_2(H_2O)]_4[Cu(en)_2]_2[Cu(H_2O)_4]_{0.5}$ $\{Cu(en)_2[H_2Ce^{IV}(\alpha\text{-}AsW_{11}O_{39})_2]_2\}\cdot 10H_2O$ (Ce: pink). (b, d and f) View of the structural unit, the 2-D sheet architecture and 2-D (6,3)-topological network of $[Cu(en)_2(H_2O)][Cu(en)_2]_{1.5}[H_3RE(\alpha\text{-}AsW_{11}O_{39})_2]^{3-}$ (RE: yellow). (g, h and i) View of the structural unit, the 2-D sheet architecture and 2-D 5-connected topological network of $[Cu(dap)_2]_{5.5}[RE(\alpha\text{-}AsW_{11}O_{39})_2]\cdot xH_2O$ (RE: rose). Cu: turquoise, WO_6: bright green, O: red, C: gray-80%, N: blue, X: light orange.

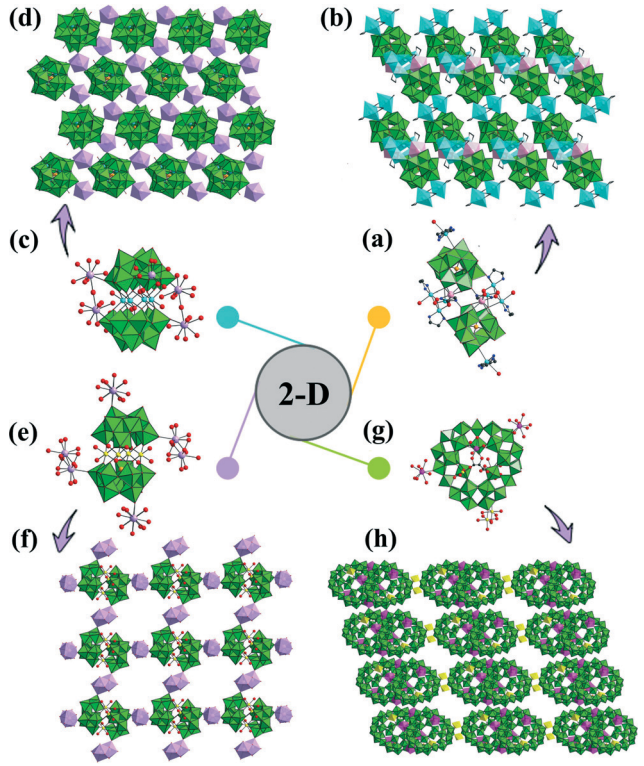

Fig. 12 (a and b) View of the structural and the 2-D sheet architecture $[Cu(en)_2][(Cu(en)(OH))_3La(SiW_{11}O_{39})]\cdot 20H_2O$ [La: rose, Cu: turquoise, C: gray-80%, N: blue, LaO_8: rose, CuO_4N_2, CuO_2N_4: turquoise]. (c and d) View of the structural unit and the 2-D sheet architecture of $\{Nd_2(H_2O)_{12}Cu_4(H_2O)_2(SiW_9O_{34})_2\}^{6-}$ [RE: lavender, Cu: turquoise, NdO_9: lavender]. (e and f) View of the structural unit and the 2-D sheet of $[Pr(H_2O)_8][Pr(H_2O)_6][Fe_4(H_2O)_{10}][B\text{-}\beta\text{-}SbW_9O_{33}]_2\cdot 16H_2O$ [Pr: lavender, Fe: yellow, PrO_8: lavender]. (g and h) View of the structural unit and the 2-D architecture of $[K_3 \subset \{GdMn(H_2O)_{10}\}\{HMnGd_2(Tart)O_2(H_2O)_{15}\}\{P_6W_{42}O_{151}(H_2O)_7\}]^{11-}$ [Gd: pink, Mn: yellow, GdO_9: pink, MnO6: yellow, C: gray-80%, N: blue]. WO_6: bright green, O: red, X: light orange.

$\{GdMn(H_2O)_{10}\}\{HMnGd_2(Tart)O_2(H_2O)_{15}\}\{P_6W_{42}O_{151}(H_2O)_7\}]^{11-}$ (Fig. 12g), which is architected from crown-shape shell $[\{WO(H_2O)\}_3(P_2W_{12}O_{48})_3]^{30-}$ units bridged by mixed TM and RE linkers ($\{Gd(H_2O)_6\}^{3+}$ and $\{Mn(H_2O)_4\}^{2+}$) was resoundingly covered by Wang's group (Fig. 12h).[18h]

The judicious selection of functional organic connectors results in achievement of the desired inorganic–organic hybrid extended structures. Besides the aforementioned 0-D, 1-D to 2-D structures, some attractive 3-D architectures have also been constructed. It should be emphasized that inorganic–organic hybrid 3-D frameworks built by 1 : 1-type and 1 : 2-type mono-RE-substituted POT units and various TM-complex cations have been produced. In 2014, Li *et al.* reported one type of 3-D PRETMHDs based on the 1 : 1-type mono-RE-substituted silicotungstate units $[Cu_{2.5}(bimpy)_2(H_2O)_2][RE(H_2O)_3(\alpha\text{-}SiW_{11}O_{39})]\cdot xH_2O$ [(RE, x) = (Eu^{3+}/Ho^{3+}/Y^{3+}, 3.5), (Sm^{3+}, 2.5), (Ce^{3+}, 3), bimpy = 3,5-bis(1-imidazolyl)pyridine] (Fig. 13a).[20j] Adjacent copper–bimpy ribbons are bridged by two antiparallel $\{-SiW_{11}O_{39}-RE-SiW_{11}O_{39}\}_n$ inorganic chains to create a 2-D sheet architecture

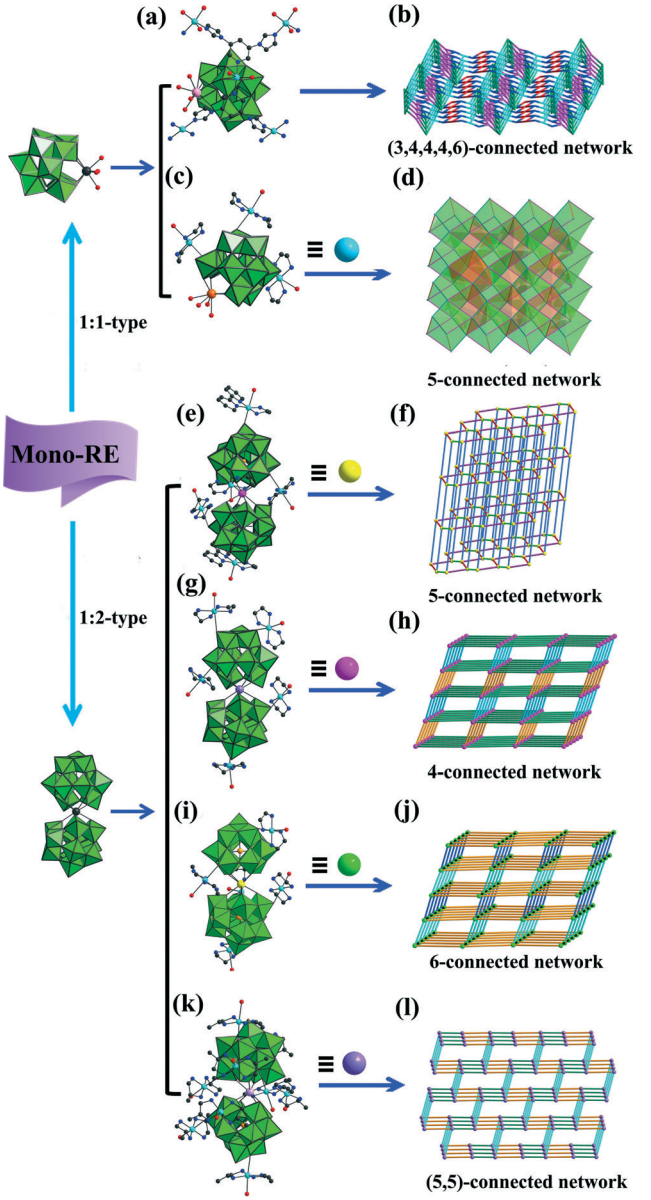

Fig. 13 (a and b) View of the structural unit and the 3-D topology of $[Cu_{2.5}(bimpy)_2(H_2O)_2][RE(H_2O)_3(\alpha\text{-}SiW_{11}O_{39})]\cdot xH_2O$ [RE: rose]. (b: Copied from ref. 20*k*). (c and d) View of the structural unit and the 3-D topology of $\{[Cu(en)_2]_{1.5}RE(\alpha\text{-}SiW_{11}O_{39})\}^{2-}$ [RE: orange]. (e and f) View of the structural unit and the 3-D topology of $\{[Cu(en)_2]_{1.5}[Cu(en)(2,2'\text{-}bpy)]Nd(\alpha\text{-}H_5PW_{11}O_{39})_2\}^{3-}$ [Nd: pink]. (g and h) View of the structural unit and the 3-D topology of $\{[Cu(en)_2(H_2O)][Cu(en)_2]_2Pr(\alpha\text{-}SiW_{11}O_{39})_2\}^{7-}$ [Pr: purple]. (i and j) View of the structural unit and the 3-D topology of $\{[Cu(en)_2(H_2O)][Cu(en)_2]_3Sm(\alpha\text{-}SiW_{11}O_{39})_2\}^{5-}$ [Sm: yellow]. (k and l) View of the structural unit and the 3-D topology of $[Cu(dap)_2]_{6.5}[RE(SiW_{11}O_{39})_2]\cdot xH_2O$ [RE: lavender]. Cu: turquoise, WO_6: bright green, O: red, C: gray-80%, N: blue, X: light orange.

and these 2-D sheets were further extended into a (3,4,4,4,6)-connected 3-D framework with $(4\cdot7^2)(4\cdot6\cdot7^3\cdot8)(4^2\cdot5^3\cdot7)(4^2\cdot7^2\cdot9^2)(4^2\cdot5^2\cdot6^7\cdot8^3\cdot10)$ topology (Fig. 13b).[20j] The other type of 3-D PRETMHDs containing 1 : 1-type mono-RE-substituted silicotungstate units could also be observed in $\{[Cu(en)_2]_{1.5}RE(\alpha\text{-}SiW_{11}O_{39})\}^{2-}$ (RE = La^{3+}, Ce^{3+}) (Fig. 13c),[20k]

which is closely related to the 2_1 screw axis to build up the unprecedented 3-D framework; this gives rise to the scarce 5-connected network with $(4^8{\cdot}6^2)$ topology (Fig. 13d) when each $\{RE(\alpha\text{-}SiW_{11}O_{39})\}^{2-}$ subunit is regarded as a 5-connected node.[20k] Furthermore, a library of fascinating 3-D PRETMHDs based on 1 : 2-type RE-substituted POT units were afforded by Niu and co-workers: (i) $\{[Cu(en)_2]_{1.5}[Cu(en)(2,2'\text{-bpy})]Nd(\alpha\text{-}H_5PW_{11}O_{39})_2\}^{3-}$ (Fig. 13e), in which each $[Nd(\alpha\text{-}PW_{11}O_{39})_2]^{11-}$ unit is linked by $[Cu(en)_2]^{2+}$ and $[Cu(en)(2,2'\text{-bpy})]^{2+}$ bridges to form the 2-D layer and neighboring layers are interconnected by O–Cu–O linkers, generating the fantastic 3-D 5-connected framework with $(4^6{\cdot}6^4)$ topology (Fig. 13f);[18d] (ii) $\{[Cu(en)_2(H_2O)][Cu(en)_2]_2Pr(\alpha\text{-}SiW_{11}O_{39})_2\}^{7-}$ (Fig. 13g), in which each $[Pr(\alpha\text{-}SiW_{11}O_{39})_2]^{13-}$ unit serves as a penta-dentate ligand to link five $[Cu(en)_2]^{2+}$ groups, giving birth to the 4-conneccted 3-D network with (6^6) topology (Fig. 13h);[20k] and (iii) $\{[Cu(en)_2(H_2O)][Cu(en)_2]_3Sm(\alpha\text{-}SiW_{11}O_{39})_2\}^{5-}$ (Fig. 13i) displaying the 3-D 6-connected $(4^8{\cdot}5^4{\cdot}6^3)$ network (Fig. 13j).[20k] Besides, Wang *et al.* obtained a group of PRETMHDs including 1 : 2-type structural units $[Cu(dap)_2]_{6.5}[RE(SiW_{11}O_{39})_2]{\cdot}xH_2O$ [(RE, x) = (Ho^{3+}/Sm^{3+}/Pr^{3+}, 9), (Dy^{3+}/Eu^{3+}/Er^{3+}, 10)] (Fig. 13k) under hydrothermal condition,[20l] in which each $[RE(\alpha\text{-}SiW_{11}O_{39})_2]^{13-}$ unit is connected to five neighboring ones through $[Cu(dap)_2]^{2+}$ cations into a 3-D 5-connected framework with the topology of $4{\cdot}4{\cdot}4{\cdot}4{\cdot}4{\cdot}4{\cdot}6_2{\cdot}6_2$ (Fig. 13l).[20l]

In 2013, Yang *et al.* successfully harvested an intricate inorganic–organic hybrid 3-D PRETMHD $\{[Ce_2(ox)_3(H_2O)_2]_2\{[Mn(H_2O)_3]_2\ [Mn_4(GeW_9O_{34})_2(H_2O)_2]\}^{8-}$ (Fig. 14a) by purposely introducing the $[A\text{-}\alpha\text{-}GeW_9O_{34}]^{10-}$ precursor into the $\{Ce^{4+}/Mn^{2+}/ox^{2-}\}$ system under hydrothermal conditions, which was established by sandwich-type tetra-Mn^{II} substituted germanotungstates through mixed Mn^{2+} and Ce^{3+} linkers.[19k] Interestingly, the sheets (Fig. 14b) constructed from sandwich-type $[Mn_4(H_2O)_2(GeW_9O_{34})_2]^{12-}$ and Mn^{2+} ions and the sheets (Fig. 14c) formed by Ce^{3+} ions and ox^{2-} bridges are alternately combined together *via* W–O–Ce–O–W generating the captivating 3-D structure (Fig. 14d), representing the first 3-D inorganic–organic hybrid PRETMHD assembled from sandwich-type TM-substituted POT fragments and mixed TM and RE linkers. Topologically, it displays a (6,8)-connected topology with a Schläfli symbol of $(3^2{\cdot}4^{12}{\cdot}5^8{\cdot}6^4{\cdot}7^2)\{3^2{\cdot}4^8{\cdot}5^2{\cdot}6^3)_2$ (Fig. 14e).[19k] To date, only a few examples of 3-D Dawson-type PRETMHDs have been communicated.[18i,j] Likewise, the hydrothermal technique has been applied to the system of TM, RE, Dawson-type POT precursor and appropriate organic ligands to prepare inorganic–organic hybrid PRETMHDs by Pang *et al.* and Yang *et al.* In 2013, Pang and collaborators added Ce^{3+} and dpdo (dpdo = 4,4′-bipyridine-*N*,*N*′-dioxide) into the preformed Mn_4-substituted $[Mn_4(H_2O)_2(P_2W_{15}O_{56})_2]^{16-}$ under hydrothermal environment, leading to a complicated 3-D POM-based metal–organic framework $\{[Ce_4(H_2O)_{22}(dpdo)_5](Mn_2HP_2W_{15}O_{56})_2\}^{2-}$ constructed from $[Mn_4(HP_2W_{15}O_{56})_2]^{14-}$ units, Ce^{3+} ions and dpdo linkers (Fig. 14g).[18i] It is fascinating that it exhibits an unusual self-penetrating topological structure, which can be symbolized as a (4,4,6)-connected network with the topology of $(4{\cdot}6^2{\cdot}8{\cdot}10^2)(4^2{\cdot}6{\cdot}8{\cdot}10^2)(4^2{\cdot}6^2{\cdot}8^9{\cdot}10^2)$ (Fig. 14h).[18i] Yang *et al.* also hydrothermally synthesized two 3-D inorganic–organic hybrid

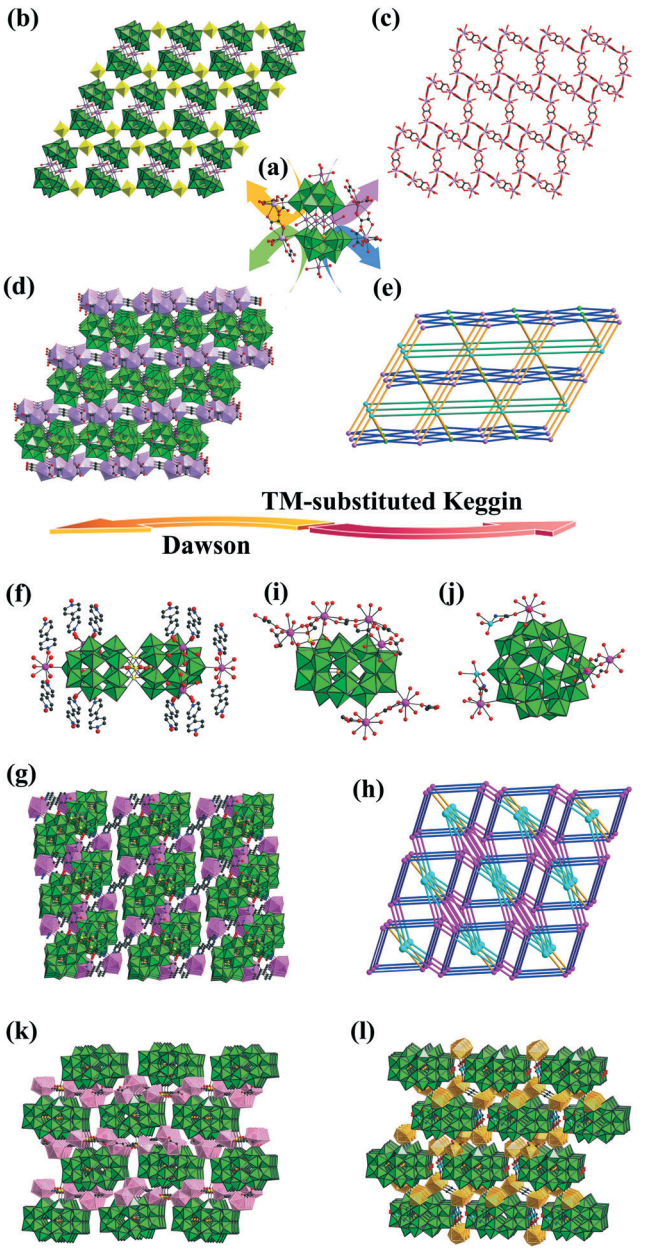

Fig. 14 (a) View of $\{[Ce_2(ox)_3(H_2O)_2]_2\{[Mn(H_2O)_3]_2[Mn_4(GeW_9O_{34})_2(H_2O)_2]\}^{8-}$ [Ce: lavender, Mn: pink]. (b) View of the sheet constructed from sandwich-type $[Mn_4(H_2O)_2(GeW_9O_{34})_2]^{12-}$ and Mn^{2+} ions [Mn: pink, MnO_6: yellow]. (c) View of the sheet formed by Ce^{3+} ions and ox^{2-} bridges [Ce: lavender]. (d) and (e) The 3-D framework and the 3-D topology of $\{[Ce_2(ox)_3(H_2O)_2]_2\{[Mn(H_2O)_3]_2[Mn_4(GeW_9\ O_{34})_2(H_2O)_2]\}^{8-}$ [Ce: lavender, Mn: pink, MnO_6: yellow, CeO_9: lavender, C: gray-80%]. (f) View of $\{[Ce_4(H_2O)_{22}(dpdo)_5](Mn_2HP_2W_{15}O_{56})_2\}^{2-}$ [Ce: pink, Mn: yellow]. (g) and (h) The 3-D framework and the 3-D topology of $\{[Ce_4(H_2O)_{22}\ (dpdo)_5](Mn_2HP_2W_{15}O_{56})_2\}^{2-}$ [Ce: pink, Mn: yellow, CeO_9: rose pink]. (i) and (k) View of the structural unit and the 3-D framework of $[\{Sm_6Mn(\mu\text{-}H_2O)_2(OCH_2COO)_7(H_2O)_{18}\}\{Na(H_2O)P_5W_{30}O_{110}\}]^{8-}$ [Sm: pink, Mn: yellow, SmO_9: rose]. (j) and (l) View of the structural unit and the 3-D framework of $[\{Sm_4Cu_2(gly)_2(ox)(H_2O)_{24}\}\{NaP_5W_{30}O_{110}\}]^{2-}$ [Sm: pink, Cu: turquoise, SmO_9: light orange]. WO_6: bright green, O: red, C: gray-80%, N: blue, X: light orange.

Preyssler $\{P_5W_{30}\}$-based PRETMHDs with TM/RE–carboxylate–RE connectors $[\{Sm_6Mn(\mu\text{-}H_2O)_2(OCH_2COO)_7(H_2O)_{18}\}\{Na(H_2O)P_5W_{30}O_{110}\}]^{8-}$ (Fig. 14i) and $[\{Sm_4Cu_2(gly)_2(ox)(H_2O)_{24}\}\{NaP_5W_{30}O_{110}\}]^{2-}$ (Fig. 14j) in sodium acetate buffer at pH = 5.5.[18j] In the structure of the former, there are three types of subunits $\{P_5W_{30}\}$, $[Sm_2Mn(\mu\text{-}H_2O)_2(OCH_2COO)_2(H_2O)_5]^{4+}$ and $[Sm_4(OCH_2COO)_5(H_2O)_{13}]^{2+}$. Adjacent $[Sm_4(OCH_2COO)_5(H_2O)_{13}]^{2+}$ subunits are combined together *via* carboxyl oxygen atoms. Each $\{P_5W_{30}\}$ subunit is connected with three $[Sm_4(OCH_2COO)_5(H_2O)_{13}]^{2+}$ subunits, while each $[Sm_4(OCH_2COO)_5(H_2O)_{13}]^{2+}$ subunit joins three $\{P_5W_{30}\}$ subunits. By this construction mode, the 2-D sheet comes into being, and then neighboring sheets are further bridged by $[Sm_2Mn(\mu\text{-}H_2O)_2(OCH_2COO)_2(H_2O)_5]^{4+}$ subunits to give rise to the 3-D framework (Fig. 14k). In the structure of the latter, there are three types of building units: $\{P_5W_{30}\}$, $[SmCu(gly)(H_2O)_8]^{4+}$ and $[Sm_2(ox)(H_2O)_8]^{4+}$ as well. Each $[SmCu(gly)(H_2O)_8]^{4+}$ subunit is connected with three $\{P_5W_{30}\}$ subunits and each $\{P_5W_{30}\}$ subunit links two $[Sm_2(ox)(H_2O)_8]^{4+}$ subunits, leading to the 3-D framework (Fig. 14l).[18j] Both are the first 3-D frameworks including $\{P_5W_{30}\}$ units and TM/RE–carboxylate–RE linkers.

In contrast to the vast number of 3d–4f heterometallic POTs mentioned above, the research on 4d–4f heterometallic POTs is still incipient and only three examples have been reported to date.[36] In this domain, the Ag^+ ion is deemed as an appropriate resource of the 4d metals considering its superiority such as the flexible coordination numbers (from two to eight) and diverse coordination geometries, the high affinity towards oxygen atoms as well as the unique argentophilicity to form $\{Ag\text{–}Ag\}_n^{2n+}$ aggregates. In 2008, Chen *et al.* discovered the first 4d–4f heterometallic POTs $[\{Ag_3(H_2O)_2\}\{Ce_2(H_2O)_{12}\} \subset \{H_2W_{11}Ce(H_2O)_4O_{39}\}_2]^{5-}$ *via* the conventional aqueous method (Fig. 15a),[36a] in which the dimeric units $[H_2W_{11}Ce(H_2O)_4O_{39}]_2^{14-}$ built by two mono-RE-substituted α-metatungstate $\{H_2W_{11}Ce(H_2O)_4O_{39}\}^{7-}$ fragments are connected by Ce^{3+} and Ag^+ linkers to generate the 2-D network, and then contiguous 2-D networks are further linked together *via* $Ag^I\text{–}Ag^I$ bonds to produce the purely inorganic 3-D framework (Fig. 15b).[36a] Later, their group hydrothermally obtained another inorganic–organic hybrid 4d–4f heterometallic POT $[Ag_6La(H_2O)_6L_4(H_2W_{12}O_{40})]^-$ (L = 2-pyrazinecarboxylic acid) (Fig. 15c), in which a La^{3+} ion is linked to four Ag–L chains and a metatungstate $\{H_2W_{12}O_{40}\}^{6-}$ unit serves as the thirteen-dentate inorganic ligand combining sixteen Ag^+ ions of six Ag–L chains, giving birth to a 3-D architecture along with La^{3+} ions (Fig. 15d).[36b] In 2013, two 4d–4f heterometallic silicotungstates $\{[Ag\{Ag_2(H_2O)_4\}\{RE(H_2O)_6\}_2 \subset \{SiW_{11}RE(H_2O)_4O_{39}\}_2]^-$ (RE = Ce^{3+}, Pr^{3+}) (Fig. 15e) were separated by Peng *et al.* by the reaction of the monovacant $[\alpha\text{-}SiW_{11}O_{39}]^{8-}$ anion with Ag^+, Ce^{3+} or Pr^{3+} ions in an aqueous solution.[36c] Intriguingly, each $[\alpha\text{-}SiW_{11}O_{39}]^{8-}$ cluster links to five Ag^+ ions and five RE^{3+} ions, delegating the highest number of connected metal atoms to any monovacant Keggin-type anion to date. Adjacent $[SiW_{11}RE(H_2O)_4O_{39}]_2^{10-}$ are in conjunction with each other by RE^{3+} and Ag^+ ions to form a 2-D lay and the fascinating 3-D structure is built by incorporating $\{Ag\text{–}Ag\}^{2+}$ aggregates into the 2-D lays (Fig. 15f).[36c] The successful isolation of these compounds not only offers attractive examples of highly connected and high-dimensional 4d–4f PRETMHDs, but also manifests the significant potential of constructing high-dimensional frameworks based on lacunary POMs and 4d–4f heterometal units in a simple synthetic strategy.

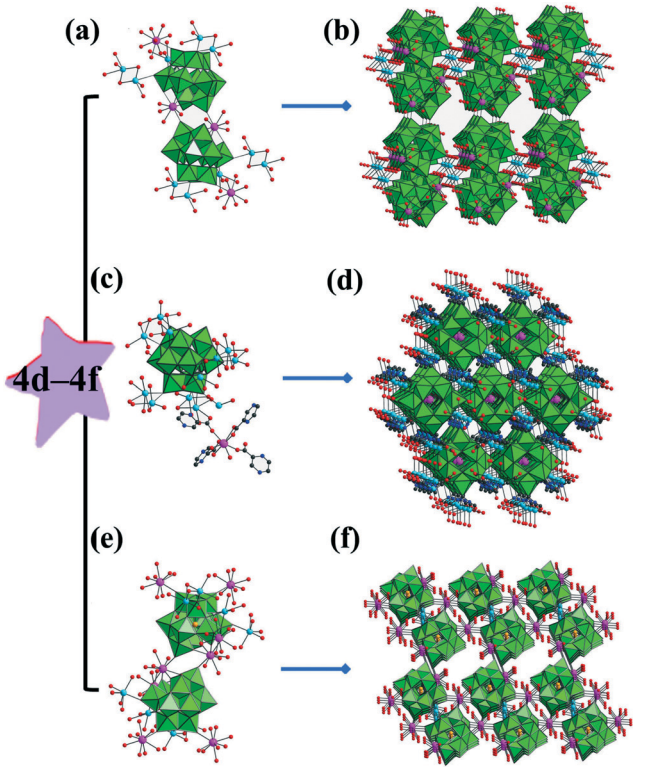

Fig. 15 (a and b) The structure unit and the 3-D framework of $[\{Ag_3(H_2O)_2\}\{Ce_2(H_2O)_{12}\}H_5 \subset \{H_2W_{11}Ce(H_2O)_4O_{39}\}_2]^{5-}$. (c and d) The structure unit and the 3-D framework of $[Ag_6La(H_2O)_6L_4(H_2W_{12}O_{40})]^-$ [C: gray-80%, N: blue]. (e and f) The structure unit and the 3-D framework of $\{[Ag\{Ag_2(H_2O)_4\}\{RE(H_2O)_6\}_2 \subset \{SiW_{11}RE(H_2O)_4O_{39}\}_2]^-$ [Si: light orange]. RE: pink, Ag: sky blue, WO_6: bright green, O: red.

5 The progress in PREREHDs

Heretofore, only one type of heterodinuclear RE-containing POTs has been reported.[37] In 2013, Mizuno and coworkers obtained a group of heterodinuclear RE-containing HMPOTs $[\{RE(\mu_2\text{-}OH)_2RE'\}(\gamma\text{-}SiW_{10}O_{36})_2]^{12-}$ (RERE′, RE = Gd^{3+}, Dy^{3+}; RE′ = Eu^{3+}, Yb^{3+}, Lu^{3+}) (Fig. 16) through the stepwise method by incorporating two types of RE ions into the vacant sites of POTs.[37] In particular, all the DyRE′ species showed the SMM behavior, and the energy barriers for magnetization reversal ($\Delta E/k_B$) of these species increased in the order of Dy–Lu (48 K) < Dy–Yb (53 K) < Dy–Dy (66 K) < Dy–Eu (73 K), which is consistent with the increasing ionic radii of RE ions adjacent to the Dy^{III} ion, which strongly demonstrates that the magnetic anisotropy of the Dy^{3+} ion and their $\Delta E/k_B$ can be manipulated by altering the coordination geometry and by

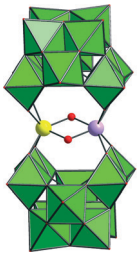

Fig. 16 The structure of $[\{RE(\mu_2\text{-}OH)_2RE'\}(\gamma\text{-}SiW_{10}O_{36})_2]^{12-}$. RE: yellow, RE′: lavender, WO_6: bright green, O: red, X: light orange.

modulating the adjacent RE′ cation in the heterodinuclear $[Dy(\mu_2\text{-}OH)_2RE']^{4+}$ cores.[37]

6 Conclusion and perspective

A comprehensive survey of HMPOTs consisting of PMGTMHDs, PTMTMHDs, PRETMHDs and PREREHDs is presented here. Evidently, the search on HMPOTs has witnessed a rapid development in the past one decade. During the course of preparation of these HMPOTs, the conventional aqueous method turns out to be an efficient synthetic method and is still widely used to create many elaborate HMPOTs. The combination of lacunary Keggin or Dawson-type precursors with TM cations in the high concentrated alkali metal salt medium is the most effective way to synthesize PMGTMHDs, while PTMTMHDs can be obtained by the substitution of alkali metal ions on PMGTMHDs with another type of TM cation. In the case of PRETMHDs, their synthetic methods can be summarized in two aspects: the self-assembly reaction of simple materials or POT precursors with metal ions and the stepwise assembly in the conventional aqueous condition including the reaction of heterometallic complexes with POT precursors, the reaction of RESP precursors with TM ions and the reaction of TMSP precursors with RE ions. The hydrothermal technique has also been explored in this field and a tremendous number of unprecedented inorganic–organic hybrid PRETMHDs with incomparable structures and aesthetic topologies have been obtained, which proves this is an effective way to make inorganic–organic hybrid PRETMHDs. In addition, by means of the stepwise assembly method, several PREREHDs have been obtained. These studies will continue to thrive because many efforts are made to develop newfangled POT derivative materials using a structure functional design viewpoint in pursuit of the structural diversities and functional applications of HMPOTs. Overall, there is still a great deal of research space for further improvement in this challenging field.

First, other synthetic methods should be introduced and deployed in the future. In the past several decades, the conventional aqueous synthetic method and the hydrothermal technology have been established as the two prominent approaches for the functionalization of POT-based materials, let alone for the construction of HMPOTs. In addition to these two synthetic strategies, synthesis using ionic liquids, ionothermal synthesis, mixed solvent diffusion method, solid-phase synthesis and microwave synthesis, which are still at their early stage in the field of POT chemistry, will be expected to be exploited in the preparation of HMPOTs. Future endeavors are anticipated to discover much more HMPOT materials with fascinating structures and attractive properties.

Second, the following attention should be also paid on varying starting materials in different reaction systems. Among the HMPOTs demonstrated in this review, most of the used POT precursors are plenary or lacunary Keggin-type, while Dawson-type precursors are less, which may be attributed to the fact that the synthetic processes for Dawson precursors is more complicated than that of Keggin precursors, the structural types of Dawson precursors are less in contrast to Keggin species, and the stability of lacunary Dawson POT fragments in the reaction system is lower than that lacunary Keggin POT fragments. In addition, during the course of preparing HMPOTs, the employed organic ligands are limited to N/O-including organic ligands and TM cations are confined to Cu^{2+}, Mn^{2+}, and Fe^{3+} cations, while other TM cations (Co^{2+}, Zn^{2+}, Ni^{2+}, Zr^{4+}, Ag^{+}, Cd^{2+}, and Cr^{3+}) are less involved. In a sense, the unicity of the starting materials may lead to the bottleneck that the majority of HMPOTs prepared are based on Keggin or Dawson POT fragments with the low-nuclear heterometal centers. Therefore, there is indeed a long way to explore well-defined synthetic conditions to achieve the aim of obtaining high-nuclear, multi-dimensional, chiral and nano-functional HMPOT materials. Thus, introduction of various precursors and diverse TM ions should attempted. Furthermore, more and more multi-functional organic components (polycarboxylic acid, polyhydroxyl, hydramine, and chiral ligands) are also needed. Undoubtedly, the interdisciplinary research by introducing other components (DNA, protein or nanoparticles) into this system will be a popular ramification in the future.

Third, the intensive and in-depth research on relevant properties of HMPOTs should be emphasized. As can be seen from the aforementioned examples, the characterization and property investigations of these species are mainly limited to solid-state properties such as IR spectroscopy, thermogravimetric analysis, powder X-ray diffraction and single-crystal X-ray diffraction, magnetism and fluorescence; however, the solution behaviors and catalytic, medicinal and conductivity properties are less involved. Hitherto, the studies of properties are comparatively superficial and not systematic. Therefore, the in-depth studies on these properties (such as infrared luminescence as well as luminescence mechanism, magnetic exchange mechanism, and thermal decomposition mechanism) should be conducted and, on the other hand, much more attention on to the solution behaviors (by means of electrospray ionization mass spectrometry, cyclic voltammetry, and nuclear magnetic resonance) and unexplored properties should be paid.

Finally, the continuous synthesis of novel HMPOTs with aesthetic structures should continue because the discovery of

new compounds is still a main driving force for developing POM chemistry. Furthermore, it is very necessary to expand heterometallic research concepts and ideology to the fields of heterometallic polyoxomolybdates, heterometallic polyoxovanadates, heterometallic polyoxoniobates or heterometallic polyoxotantates, which will dramatically widen and enrich the research categories of POMs. Thus, we believe there are very fruitful avenues for future development of heterometallic POMs.

Abbreviations

HMPOT	Heterometallic polyoxotungstate
MG	Main-group
TM	Transition-metal
RE	Rare-earth
POM	Polyoxometalate
POT	Polyoxotungstate
PMGTMHDs	POT-based MG and TM heterometallic derivatives
PTMTMHDs	POT-based TM and TM heterometallic derivatives
PRETMHDs	POT-based RE and TM heterometallic derivatives
PREREHDs	POT-based RE and RE heterometallic derivatives TMSPs TM-substituted POTs
RESPs	RE-substituted POTs
CV	Cyclic voltammetry
THF	Tetrahydrofuran
en	Ethylenediamine
dap	1,2-Diaminopropane
2,2′-bpy	2,2′-Bipyridine
pzda	Pyrazine-2,3-dicarboxylate
thr	Threonine
ox	Oxalate
Cp	Cyclopentadienyl
H_5Ale	Alendronic acid
im	Imidazole
TBA	Tetrabutylammonium
Tart	Tartate
bimpy	3,5-Bis(1-imidazolyl)pyridine
dpdo	4,4′-Bipyridine-*N*,*N*′-dioxide
gly	Glycine

Acknowledgements

This study was sponsored by the Natural Science Foundation of China (21301049, U1304208, 21571048), Program for Science & Technology Innovation Talents in Universities of Henan Province (16HASTIT001), the Natural Science Foundation of Henan Province (122300410106, 142300410451), the Postdoctoral Foundation of Henan Province, 2014 Special Foundation for Scientific Research Project of Henan University (XXJC20140001), 2012 Young Backbone Teachers Foundation from Henan Province (2012GGJS-027) and the Students Innovative Pilot Plan of Henan University (15NA002).

Notes and references

1 (*a*) Q. Yin, J. M. Tan, C. Besson, Y. V. Geletii, D. G. Musaev, A. E. Kuznetsov, Z. Luo, K. I. Hardcastle and C. L. Hill, *Science*, 2010, **328**, 342; (*b*) J. M. Clemente-Juan, E. Coronado and A. Gaita-Arino, *Chem. Soc. Rev.*, 2012, **41**, 7464; (*c*) D. L. Long, R. Tsunashima and L. Cronin, *Angew. Chem., Int. Ed.*, 2010, **49**, 1736; (*d*) J. Berzelius and J. Pogg, *Ann. Phys.*, 1826, **6**, 369; (*e*) C. L. Hill, *Chem. Rev.*, 1998, **98**, 1; (*f*) J. T. Rhule, C. L. Hill, D. A. Judd and R. F. Schinazi, *Chem. Rev.*, 1998, **98**, 327; (*g*) C. J. Jiang, A. Lesbani, R. Kawamoto, S. Uchida and N. Mizuno, *J. Am. Chem. Soc.*, 2006, **128**, 14240; (*h*) Y. Wang, L. Ye, T. G. Wang, X. B. Cui, S. Y. Shi, G. W. Wang and J. Q. Xu, *Dalton Trans.*, 2010, **39**, 1916; (*i*) U. Kortz, A. Müller, J. van Slageren, J. Schnack, N. S. Dalal and M. Dressel, *Coord. Chem. Rev.*, 2009, **253**, 2315; (*j*) S. T. Zheng and G. Y. Yang, *Chem. Soc. Rev.*, 2012, **41**, 7623; (*k*) Y. Wang and I. A. Weinstock, *Chem. Soc. Rev.*, 2012, **41**, 7479.

2 (*a*) W. L. Chen, Y. G. Li, Y. H. Wang, E. B. Wang and Z. M. Zhang, *Dalton Trans.*, 2008, 865; (*b*) J. P. Wang, W. Wang and J. Y. Niu, *J. Mol. Struct.*, 2008, **873**, 29; (*c*) A. Merca, A. Müller, J. van Slageren, M. Läge and B. Krebs, *J. Cluster Sci.*, 2007, **18**, 711.

3 (*a*) Z. M. Zhang, Y. G. Li, S. Yao and E. B. Wang, *Dalton Trans.*, 2011, **40**, 6475; (*b*) Y. W. Li, Y. G. Li, Y. H. Wang, X. J. Feng, Y. Lu and E. B. Wang, *Inorg. Chem.*, 2009, **48**, 6452; (*c*) H. H. Wu, S. Yao, Z. M. Zhang, Y. G. Li, Y. Song, Z. J. Liu, X. B. Han and E. B. Wang, *Dalton Trans.*, 2013, **42**, 342.

4 (*a*) C. M. Tourn, G. F. Tourn and F. Zonnevijlle, *J. Chem. Soc., Dalton Trans.*, 1991, 143; (*b*) R. Neumann and A. M. Khenkin, *Inorg. Chem.*, 1995, **34**, 5753; (*c*) R. Cao, K. P. O'Halloran, D. A. Hillesheim, S. Lense, K. I. Hardcastle and C. L. Hill, *CrystEngComm*, 2011, **13**, 738.

5 V. E. Simmons and L. C. W. Baker, *Proc. VII I.C.C.C.*, Stockholm, 1962, p. 195.

6 L. C. W. Baker and V. E. Simmons, *Proc. IX I.C.C.C.*, St. Moritz, 1966, p. 421.

7 (*a*) D. E. Katsoulis and M. T. Pope, *J. Am. Chem. Soc.*, 1984, **106**, 2737; (*b*) L. S. Felices, P. Vitoria, J. M. Gutiérrez Zorrilla, L. Lezama and S. Reinoso, *Inorg. Chem.*, 2006, **45**, 7748; (*c*) V. Lahootun, C. Besson, R. Villanneau, F. Villain, L. M. Chamoreau, K. Boubekeur, S. Blanchard, R. Thouvenot and A. Proust, *J. Am. Chem. Soc.*, 2007, **129**, 7127; (*d*) F. Hussain, B. S. Bassil, L. H. Bi, M. Reicke and U. Kortz, *Angew. Chem., Int. Ed.*, 2004, **43**, 3485; (*e*) P. Mialane, A. Dolbecq, J. Marrot, E. Rivière and F. Sécheresse, *Chem. – Eur. J.*, 2005, **11**, 1771; (*f*) S. T. Zheng, D. Q. Yuan, H. P. Jia, J. Zhang and G. Y. Yang, *Chem. Commun.*, 2007, 1858; (*g*) X. X. Li, W. H. Fang, J. W. Zhao and G. Y. Yang, *Chem. – Eur. J.*, 2015, **21**, 2315.

8 T. J. R. Weakley, H. T. Evans, Jun., J. S. Showell, G. F. Tourné and C. M. Tourné, *J. Chem. Soc., Chem. Commun.*, 1973, 139.

9 R. G. Finke and M. W. Droege, *Inorg. Chem.*, 1983, **22**, 1006.

10 S. H. Wasfi, A. L. Rheingold, G. F. Kokoszka and A. S. Goldstein, *Inorg. Chem.*, 1987, **26**, 2934.

11 (*a*) B. Keita and L. Nadjo, in *Encyclopedia of Electrochemistry: Electrochemistry of Isopoly and Heteropoly Oxometalates*, ed. A. J. Bard and M. Stratmann, Wiley-VCH, Weinheim, 2006, vol. 7, p. 607; (*b*) B. Keita and L. Nadjo, *J. Mol. Catal. A: Chem.*, 2007, **262**, 190.

12 G. A. Barbieri, *Atti. Accad. Naz. Lincei*, 1914, **11**, 805.

13 (*a*) R. D. Peacock and T. J. R. Weakley, *J. Chem. Soc. A*, 1971, 1836; (*b*) A. V. Botar and T. J. R. Weakley, *Rev. Roum. Chim.*, 1973, **18**, 1155.

14 M. Sadakane, M. H. Dickman and M. T. Pope, *Angew. Chem., Int. Ed.*, 2000, **39**, 2914.

15 (*a*) B. S. Bassil, M. H. Dickman, I. Römer, B. von der Kammer and U. Kortz, *Angew. Chem., Int. Ed.*, 2007, **46**, 6192; (*b*) F. Hussain, F. Conrad and G. R. Patzke, *Angew. Chem., Int. Ed.*, 2009, **48**, 9088; (*c*) K. Y. Cui, F. Y. Li, L. Xu, B. B. Xu, N. Jiang, Y. C. Wang and J. Zhang, *Dalton Trans.*, 2012, **41**, 4871; (*d*) L. B. Ni, F. Hussain, B. Spingler, S. Weyeneth and G. R. Patzke, *Inorg. Chem.*, 2011, **50**, 4944; (*e*) K. Wassermann, M. H. Dickman and M. T. Pope, *Angew. Chem., Int. Ed. Engl.*, 1997, **36**, 1445.

16 (*a*) L. Y. Song, D. D. Zhang, P. T. Ma, Z. J. Liang, J. P. Wang and J. Y. Niu, *CrystEngComm*, 2013, **15**, 4597; (*b*) W. C. Chen, H. L. Li, X. L. Wang, K. Z. Shao, Z. M. Su and E. B. Wang, *Chem. – Eur. J.*, 2013, **19**, 11007; (*c*) W. C. Chen, X. L. Wang, Y. Q. Jiao, P. Huang, E. L. Zhou, Z. M. Su and K. Z. Shao, *Inorg. Chem.*, 2014, **53**, 9486.

17 G. L. Xue, B. Liu, H. M. Hu, J. H. Yang, J. W. Wang and F. Fu, *J. Mol. Struct.*, 2004, **690**, 95.

18 (*a*) X. K. Fang and P. Köegerler, *Chem. Commun.*, 2008, 3396; (*b*) X. K. Fang and P. Kögerler, *Angew. Chem., Int. Ed.*, 2008, **47**, 8123; (*c*) A. H. Ismail, B. S. Bassil, G. H. Yassin, B. Keita and U. Kortz, *Chem. – Eur. J.*, 2012, **18**, 6163; (*d*) J. Y. Niu, S. W. Zhang, H. N. Chen, J. W. Zhao, P. T. Ma and J. P. Wang, *Cryst. Growth Des.*, 2011, **11**, 3769; (*e*) J. F. Cao, S. X. Liu, R. G. Cao, L. H. Xie, Y. H. Ren, C. Y. Gao and L. Xu, *Dalton Trans.*, 2008, 115; (*f*) H. Y. Zhao, J. W. Zhao, B. F. Yang, H. He and G. Y. Yang, *CrystEngComm*, 2014, **16**, 2230; (*g*) H. Y. Zhao, J. W. Zhao, B. F. Yang, H. He and G. Y. Yang, *CrystEngComm*, 2013, **15**, 5209; (*h*) S. Yao, Z. M. Zhang, Y. G. Li, Y. Lu, E. B. Wang and Z. M. Su, *Cryst. Growth Des.*, 2010, **10**, 135; (*i*) T. T. Yu, H. Y. Ma, C. J. Zhang, H. J. Pang, S. B. Li and H. Liu, *Dalton Trans.*, 2013, **42**, 16328; (*j*) Y. Y. Li, J. W. Zhao, Q. Wei, B. F. Yang, H. He and G. Y. Yang, *Chem. – Asian J.*, 2014, **9**, 858; (*k*) Y. Y. Li, S. B. Tian, Y. Z. Li, J. W. Zhao, P. T. Ma and L. J. Chen, *Inorg. Chim. Acta*, 2013, **405**, 105; (*l*) D. Y. Shi, L. J. Chen, J. W. Zhao, Y. Wang, P. T. Ma and J. Y. Niu, *Inorg. Chem. Commun.*, 2011, **14**, 324; (*m*) S. S. Shang, J. W. Zhao, L. J. Chen, Y. Y. Li, J. L. Zhang, Y. Z. Li and J. Y. Niu, *J. Solid State Chem.*, 2012, **196**, 29; (*n*) L. J. Chen, D. Y. Shi, Y. Wang, H. L. Chen, Z. D. Geng, J. W. Zhao, P. T. Ma and J. Y. Niu, *J. Coord. Chem.*, 2011, **64**, 400.

19 (*a*) S. Reinoso and J. R. Galán-Mascarós, *Inorg. Chem.*, 2010, **49**, 377; (*b*) J. W. Zhao, D. Y. Shi, L. J. Chen, Y. Z. Li, P. T. Ma, J. P. Wang and J. Y. Niu, *Dalton Trans.*, 2012, **41**, 10740; (*c*) S. Reinoso, J. R. Galán-Mascarós and L. Lezama, *Inorg. Chem.*, 2011, **50**, 9587; (*d*) J. L. Zhang, J. Li, L. J. Li, H. Z. Zhao, P. T. Ma, J. W. Zhao and L. J. Chen, *Spectrochim. Acta, Part A*, 2013, **114**, 360; (*e*) J. Wang, J. W. Zhao, H. Y. Zhao, B. F. Yang, H. He and G. Y. Yang, *CrystEngComm*, 2014, **16**, 252; (*f*) S. Reinoso, M. Giménez-Marqués, J. R. Galán-Mascarós, P. Vitoria and J. M. Gutiérrez-Zorrilla, *Angew. Chem., Int. Ed.*, 2010, **49**, 8384; (*g*) M. Ibrahim, V. Mereacre, N. Leblanc, W. Wernsdorfer, C. E. Anson and A. K. Powell, *Angew. Chem., Int. Ed.*, 2015, **54**, 15574; (*h*) J. P. Wang, Q. X. Yan, X. D. Du and J. Y. Niu, *J. Cluster Sci.*, 2008, **19**, 491; (*i*) J. W. Zhao, D. Y. Shi, L. J. Chen, P. T. Ma, J. P. Wang, J. Zhang and J. Y. Niu, *Cryst. Growth Des.*, 2013, **13**, 4368; (*j*) J. W. Zhao, Y. Z. Li, F. Ji, J. Yuan, L. J. Chen and G. Y. Yang, *Dalton Trans.*, 2014, **43**, 5694; (*k*) H. Y. Zhao, J. W. Zhao, B. F. Yang, H. He and G. Y. Yang, *Cryst. Growth Des.*, 2013, **13**, 5169.

20 (*a*) Y. Z. Chen, Z. J. Liu, Z. M. Zhang, H. Y. Zhou, X. T. Zheng and E. B. Wang, *Inorg. Chem. Commun.*, 2014, **46**, 155; (*b*) S. W. Zhang, J. W. Zhao, P. T. Ma, J. Y. Niu and J. P. Wang, *Chem. – Asian J.*, 2012, **7**, 966; (*c*) H. Y. Zhao, J. W. Zhao, B. F. Yang, H. He and G. Y. Yang, *CrystEngComm*, 2013, **15**, 8186; (*d*) X. K. Fang, K. McCallum, H. D. Pratt III, T. M. Anderson, K. Dennis and M. Luban, *Dalton Trans.*, 2012, **41**, 9867; (*e*) D. Y. Du, J. S. Qin, S. L. Li, Y. Q. Lan, X. L. Wang and Z. M. Su, *Aust. J. Chem.*, 2010, **63**, 1389; (*f*) J. D. Compain, P. Mialane, A. Dolbecq, I. M. Mbomekallé, J. Marrot, F. Sécheresse, C. Duboc and E. Rivière, *Inorg. Chem.*, 2010, **49**, 2851; (*g*) W. L. Chen, Y. G. Li, Y. H. Wang and E. B. Wang, *Eur. J. Inorg. Chem.*, 2007, 2216; (*h*) B. Nohra, P. Mialane, A. Dolbecq, E. Rivière, J. Marrot and F. Sécheresse, *Chem. Commun.*, 2009, 2703; (*i*) Z. M. Zhang, Y. G. Li, W. L. Chen, E. B. Wang and X. L. Wang, *Inorg. Chem. Commun.*, 2008, **11**, 879; (*j*) W. L. Zhou, Z. Y. Zhang, J. Peng, X. Wang, Z. Y. Shi and G. Z. Li, *CrystEngComm*, 2014, **16**, 10893; (*k*) S. W. Zhang, J. W. Zhao, P. T. Ma, H. N. Chen, J. Y. Niu and J. P. Wang, *Cryst. Growth Des.*, 2012, **12**, 1263; (*l*) S. Yao, J. H. Yan, H. D. Z. M. Zhang, Y. G. Li, X. B. Han, J. Q. Shen, H. Fu and E. B. Wang, *Eur. J. Inorg. Chem.*, 2013, 4770; (*m*) S. Yao, J. H. Yan, Y. C. Yu and E. B. Wang, *Inorg. Chem. Commun.*, 2012, **23**, 70; (*n*) J. Luo, J. W. Zhao, J. Yuan, Y. Z. Li, L. J. Chen, P. T. Ma, J. P. Wang and J. Y. Niu, *Inorg. Chem. Commun.*, 2013, **27**, 13; (*o*) D. D. Zhang, S. W. Zhang, P. T. Ma, J. P. Wang and J. Y. Niu, *Inorg. Chem. Commun.*, 2012, **20**, 191.

21 (*a*) W. L. Chen, Y. G. Li, Y. H. Wang, E. B. Wang and Z. M. Su, *Dalton Trans.*, 2007, 4293; (*b*) L. J. Chen, F. Zhang, X. Ma, J. Luo and J. W. Zhao, *Dalton Trans.*, 2015, **44**, 12598; (*c*) D. Y. Shi, J. W. Zhao, L. J. Chen, P. T. Ma, J. P. Wang and J. Y. Niu, *CrystEngComm*, 2012, **14**, 3108; (*d*) D. Y. Shi, S. S. Shang, L. J. Chen, X. M. Cai, X. Y. Wang and J. W. Zhao, *Synth. Met.*, 2012, **162**, 1030.

22 (*a*) J. W. Zhao, J. Zhang, S. T. Zheng and G. Y. Yang, *Inorg. Chem.*, 2007, **46**, 10944; (*b*) J. W. Zhao, C. M. Wang, J. Zhang, S. T. Zheng and G. Y. Yang, *Chem. – Eur. J.*, 2008, **14**, 9223; (*c*) J. W. Zhao, J. Zhang, S. T. Zheng and G. Y. Yang,

Chem. Commun., 2008, 570; (*d*) J. W. Zhao, J. Zhang, Y. Song, S. T. Zheng and G. Y. Yang, *Eur. J. Inorg. Chem.*, 2008, 3809; (*e*) S. T. Zheng, J. Zhang and G. Y. Yang, *Angew. Chem., Int. Ed.*, 2008, **47**, 3909; (*f*) S. T. Zheng, J. Zhang, J. M. Clemente-Juan, D. Q. Yuan and G. Y. Yang, *Angew. Chem., Int. Ed.*, 2009, **48**, 7176; (*g*) S. T. Zheng, J. Zhang, X. X. Li, W. H. Fang and G. Y. Yang, *J. Am. Chem. Soc.*, 2010, **132**, 15102; (*h*) X. X. Li, S. T. Zheng, J. Zhang, W. H. Fang, G. Y. Yang and J. M. Clemente-Juan, *Chem. – Eur. J.*, 2011, **17**, 13032; (*i*) J. W. Zhao, D. Y. Shi, L. J. Chen, X. M. Cai, Z. Q. Wang, P. T. Ma, J. P. Wang and J. Y. Niu, *CrystEngComm*, 2012, **14**, 2797; (*j*) J. W. Zhao, D. Y. Shi, L. J. Chen, P. T. Ma, J. P. Wang and J. Y. Niu, *CrystEngComm*, 2011, **13**, 3462; (*k*) C. Pichon, A. Dolbecq, P. Mialane, J. Marrot, E. Rivièreb and F. Sécheresse, *Dalton Trans.*, 2008, 71; (*l*) C. Pichon, A. Dolbecq, P. Mialane, J. Marrot, E. Rivière, M. Goral, M. Zynek, T. McCormac, S. A. Borshch, E. Zueva and F. Sécheresse, *Chem. – Eur. J.*, 2008, **14**, 3189.

23 (*a*) J. W. Zhao, H. P. Jia, J. Zhang, S. T. Zheng and G. Y. Yang, *Chem. – Eur. J.*, 2007, **13**, 10030; (*b*) R. A. Laudise, *Prog. Inorg. Chem.*, 1962, **3**, 1; (*c*) A. Rabenau, *Angew. Chem., Int. Ed. Engl.*, 1985, **24**, 1026; (*d*) R. A. Laudise, *Chem. Eng. News*, 1987, **65**, 30; (*e*) P. J. Hagrman, D. Hagrman and J. Zubietua, *Angew. Chem., Int. Ed.*, 1999, **38**, 2638.

24 (*a*) U. Kortz, I. M. Mbomekalle, B. Keita, L. Nadjo and P. Berthet, *Inorg. Chem.*, 2002, **41**, 6412; (*b*) I. M. Mbomekalle, B. Keita, L. Nadjo and P. Berthet, *Inorg. Chem. Commun.*, 2003, **6**, 435; (*c*) L. Ruhlmann, J. Canny, R. Contant and R. Thouvenot, *Inorg. Chem.*, 2002, **41**, 3811; (*d*) J. M. Clemente-Juan, E. Coronado, A. Gaita-Arino, C. Gimenez-Saiz, H.-U. Gudel, A. Sieber, R. Bircher and H. Mutka, *Inorg. Chem.*, 2005, **44**, 3389; (*e*) D. Schaming, J. Canny, K. Boubekeur, R. Thouvenot and L. Ruhlmann, *Eur. J. Inorg. Chem.*, 2009, 5004; (*f*) L. Ruhlmann, C. Costa-Coquelard, J. Canny and R. Thouvenot, *J. Electroanal. Chem.*, 2007, **603**, 260; (*g*) X. Zhang, T. M. Anderson, Q. Chen and C. L. Hill, *Inorg. Chem.*, 2001, **40**, 418; (*h*) Y. Hou, L. Xu, M. J. Cichon, S. Lense, K. I. Hardcastle and C. L. Hill, *Inorg. Chem.*, 2010, **49**, 4125; (*i*) T. M. Anderson, X. K. Fang, I. M. Mbomekalle, B. Keita, L. Nadjo, K. I. Hardcastle, A. Farsidjani and C. L. Hill, *J Cluster Sci.*, 2006, **17**, 183; (*j*) T. M. Anderson, X. Zhang, K. I. Hardcastle and C. L. Hill, *Inorg. Chem.*, 2002, **41**, 2477; (*k*) B. Keita, I. M. Mbomekalle, L. Nadjo, T. M. Anderson and C. L. Hill, *Inorg. Chem.*, 2004, **43**, 3275; (*l*) M. Lebrini, I. M. Mbomekalle, A. Dolbecq, J. Marrot, P. Berthet, J. Ntienoue, F. Sécheresse, J. Vigneron and A. Etcheberry, *Inorg. Chem.*, 2011, **50**, 6437; (*m*) G. B. Zhu, Y. V. Geletii, J. Song, C. C. Zhao, E. N. Glass, J. Bacsa and C. L. Hill, *Inorg. Chem.*, 2013, **52**, 1018; (*n*) N. Laronze, J. Marrot and G. Hervé, *Inorg. Chem.*, 2003, **42**, 5857; (*o*) Y. L. Liu, J. Cao, Y. J. Wang, Y. Z. Li, J. W. Zhao, L. J. Chen, P. T. Ma and J. Y. Niu, *J. Solid State Chem.*, 2014, **209**, 113; (*p*) U. Kortz, N. K. Al-Kassem, M. G. Savelieff, N. A. Al Kadi and M. Sadakane, *Inorg. Chem.*, 2001, **40**, 4742; (*q*) A. C. Stowe, S. Nellutla, N. S. Dalal and U. Kortz, *Eur. J. Inorg. Chem.*, 2004, 3792; (*r*) H. Liu, L. Xu, G. G. Gao, F. Y. Li and N. Jiang, *J. Mol. Struct.*, 2008, **878**, 124; (*s*) H. Liu, Y. Liu, H. Y. Liu, C. H. Shi, F. H. Liu and H. L. Liu, *Inorg. Chem. Commun.*, 2009, **12**, 1; (*t*) L. H. Bi, M. Reicke, U. Kortz, B. Keita, L. Nadjo and R. J. Clark, *Inorg. Chem.*, 2004, **43**, 3915; (*u*) L. H. Bi, U. Körtz, B. Keita, L. Nadjo and H. Borrmann, *Inorg. Chem.*, 2004, **43**, 8367; (*v*) L. H. Bi, U. Körtz, B. Keita, L. Nadjo and L. Daniels, *Eur. J. Inorg. Chem.*, 2005, 3034.

25 (*a*) X. J. Sang, J. S. Li, L. C. Zhang, Z. J. Wang, W. L. Chen, Z. M. Zhu, Z. M. Su and E. B. Wang, *ACS Appl. Mater. Interfaces*, 2014, **6**, 7876; (*b*) X. J. Sang, J. S. Li, L. C. Zhang, Z. M. Zhu, W. L. Chen, Y. G. Li, Z. M. Su and E. B. Wang, *Chem. Commun.*, 2014, **50**, 14678; (*c*) B. Zhang, L. C. Zhang, Y. J. Zhang, F. Su, W. S. You and Z. M. Zhu, *RSC Adv.*, 2015, **5**, 47319; (*d*) Z. J. Wang, L. C. Zhang, Z. M. Zhu, W. L. Chen, W. S. You and E. B. Wang, *Inorg. Chem. Commun.*, 2012, **17**, 151; (*e*) C. N. Kato, Y. Makino, W. Unnoa and H. Uno, *Dalton Trans.*, 2013, **42**, 1129.

26 (*a*) H. Liu, C. Qin, Y. G. Wei, L. Xu, G. G. Gao, F. Y. Li and X. S. Qu, *Inorg. Chem.*, 2008, **47**, 4166; (*b*) J. P. Wang, P. T. Ma, J. Li, H. Y. Niu and J. Y. Niu, *Chem. – Asian J.*, 2008, **3**, 822; (*c*) U. Kortz, S. Nellutla, A. C. Stowe, N. S. Dalal, J. V. Tol and B. S. Bassil, *Inorg. Chem.*, 2004, **43**, 144; (*d*) X. L. Xue, X. F. Zhao, D. S. Zhang, Z. G. Han, H. G. Yu and X. L. Zhai, *RSC Adv.*, 2014, **4**, 63670.

27 (*a*) I. M. Mbomekalle, P. Mialane, A. Dolbecq, J. Marrot, F. Sécheresse, P. Berthet, B. Keita and L. Nadjo, *Eur. J. Inorg. Chem.*, 2009, 5194; (*b*) L. Ruhlmann, J. Canny, J. Vaissermann and R. Thouvenot, *Dalton Trans.*, 2004, 794; (*c*) I. M. Mbomekalle, B. Keita, L. Nadjo, W. A. Neiwert, L. Zhang, K. I. Hardcastle, C. L. Hill and T. M. Anderson, *Eur. J. Inorg. Chem.*, 2003, 3924; (*d*) X. Zhang and C. L. Hill, *Chem. Ind.*, 1998, **75**, 519; (*e*) L. Ruhlmann, C. Costa-Coquelard, J. Canny and R. Thouvenot, *Eur. J. Inorg. Chem.*, 2007, 1493; (*f*) I. M. Mbomekalle, R. Cao, K. I. Hardcastle, C. L. Hill, M. Ammam, B. Keita, L. Nadjo and T. M. Anderson, *C. R. Chim.*, 2005, **8**, 1077; (*g*) F. Doungmene, P. A. Aparicio, J. Ntienoue, C. S. A. Mezui, P. de Oliveira, X. López and I. M. Mbomekalle, *Electrochim. Acta*, 2014, **125**, 674; (*h*) T. M. Anderson, K. I. Hardcastle, N. Okun and C. L. Hill, *Inorg. Chem.*, 2001, **40**, 6418; (*i*) I. V. Kalinina, N. V. Izarova and U. Kortz, *Inorg. Chem.*, 2012, **51**, 7442; (*j*) L. H. Bi, G. F. Hou, L. X. Wu and U. Kortz, *CrystEngComm*, 2009, **11**, 1532; (*k*) R. Q. Meng, L. Suo, G. F. Hou, J. Liang, L. H. Bi, H. L. Li and L. X. Wu, *CrystEngComm*, 2013, **15**, 5867; (*l*) K. Suzuki, Y. Kikukawa, S. Uchida, H. Tokoro, K. Imoto, S. Ohkoshi and N. Mizuno, *Angew. Chem., Int. Ed.*, 2012, **51**, 1597.

28 I. M. Mbomekalle, B. Keita, M. Nierlich, U. Kortz, P. Berthet and L. Nadjo, *Inorg. Chem.*, 2003, **42**, 5143.

29 L. X. Shi, W. F. Zhao, X. Xu, J. Tang and C. D. Wu, *Inorg. Chem.*, 2011, **50**, 12387.

30 (*a*) A. J. Tasiopoulos, T. A. O'Brien, K. A. Abboud and G. Christou, *Angew. Chem., Int. Ed.*, 2004, **43**, 345; (*b*) A. J. Tasiopoulos, P. L. Milligan, Jr., K. A. Abboud, T. A. O'Brien and G. Christou, *Inorg. Chem.*, 2007, **46**, 9678.

31 L. J. Chen, J. Cao, X. H. Li, X. Ma, J. Luo and J. W. Zhao, *CrystEngComm*, 2015, **17**, 5002.
32 S. Yao, J. H. Yan, H. Duan, Q. Q. Jia, Z. M. Zhang and E. B. Wang, *RSC Adv.*, 2015, **5**, 76206.
33 (*a*) M. L. Kahn, C. Mathonière and O. Kahn, *Inorg. Chem.*, 1999, **38**, 3692; (*b*) M. Andruh, I. Ramade, E. Codjovi, O. Guillou, O. Kahn and J. C. Trombe, *J. Am. Chem. Soc.*, 1993, **115**, 1822; (*c*) O. Kahn and O. Guillou, in *New Frontiers in Magnetochemistry*, ed. C. J. O'Connor, World Scientific, Singapore, 1993; (*d*) J. P. Costes, F. Dahan, A. Dupuis and J. P. Laurent, *Chem. – Eur. J.*, 1998, **4**, 1616.
34 J. W. Zhao, J. Cao, Y. Z. Li, J. Zhang and L. J. Chen, *Cryst. Growth Des.*, 2014, **14**, 6217.
35 T. Lis, *Acta Crystallogr., Sect. B: Struct. Crystallogr. Cryst. Chem.*, 1980, **36**, 2042.
36 (*a*) H. J. Pang, C. J. Zhang, D. M. Shi and Y. G. Chen, *Cryst. Growth Des.*, 2008, **8**, 4476; (*b*) Y. Lv, Y. G. Chen and X. M. Li, *Inorg. Chem. Commun.*, 2014, **45**, 33; (*c*) H. J. Pang, C. J. Gómez-García, J. Peng, H. Y. Ma, C. J. Zhang and Q. Y. Wu, *Dalton Trans.*, 2013, **42**, 16596.
37 R. Sato, K. Suzuki, M. Sugawa and N. Mizuno, *Chem. – Eur. J.*, 2013, **19**, 12982.

